

Studying stars at the reionization epoch with gravitational lensing

Jose M. Diego

Instituto de Física de Cantabria (CSIC-UC), Santander, Spain



GOBIERNO
DE ESPAÑA

MINISTERIO
DE CIENCIA, INNOVACIÓN
Y UNIVERSIDADES



CONSEJO SUPERIOR DE INVESTIGACIONES CIENTÍFICAS



Instituto de Física de Cantabria



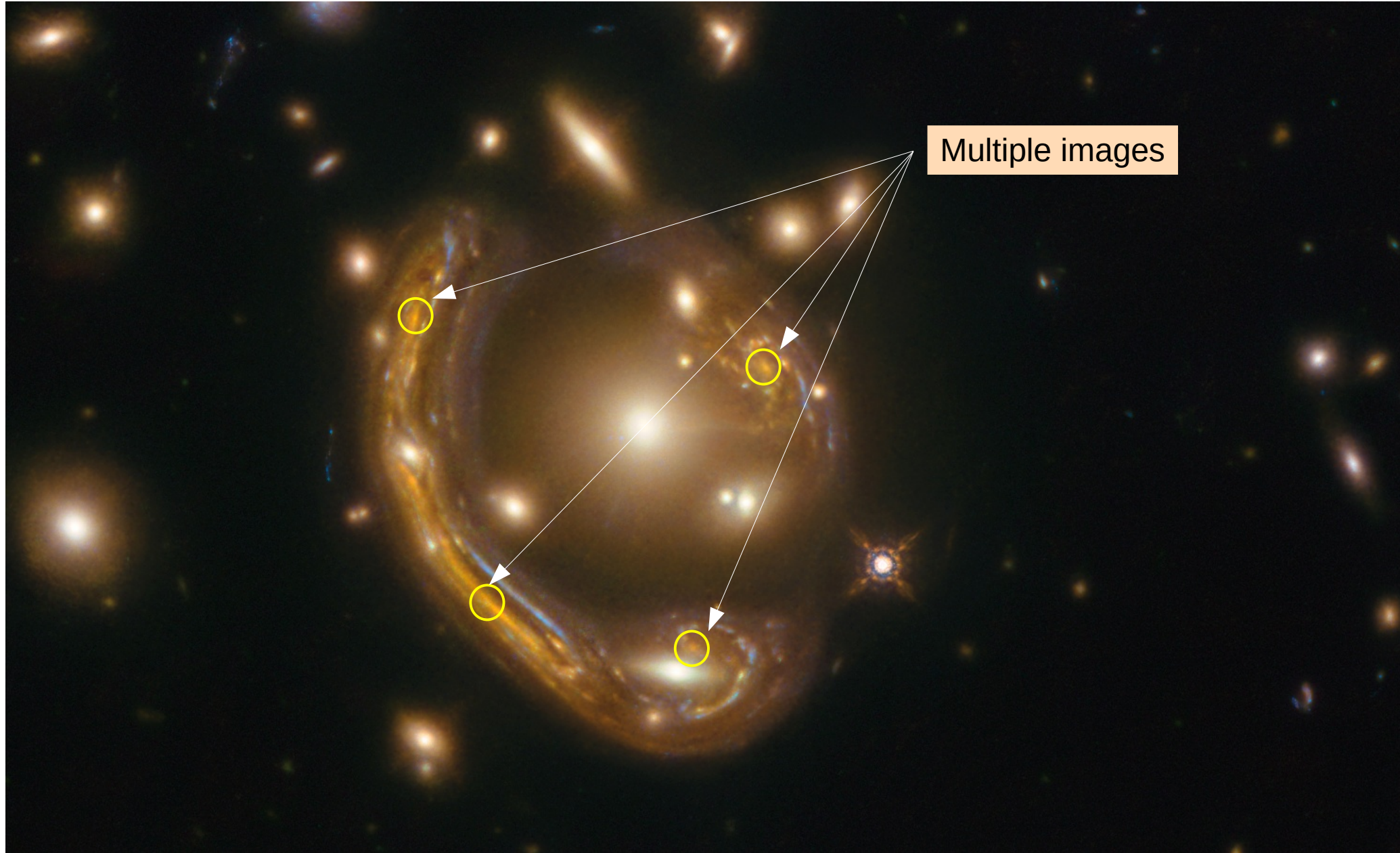
EXCELENCIA
MARÍA
DE MAEZTU

TIFR Mumbai
April 1st 2022

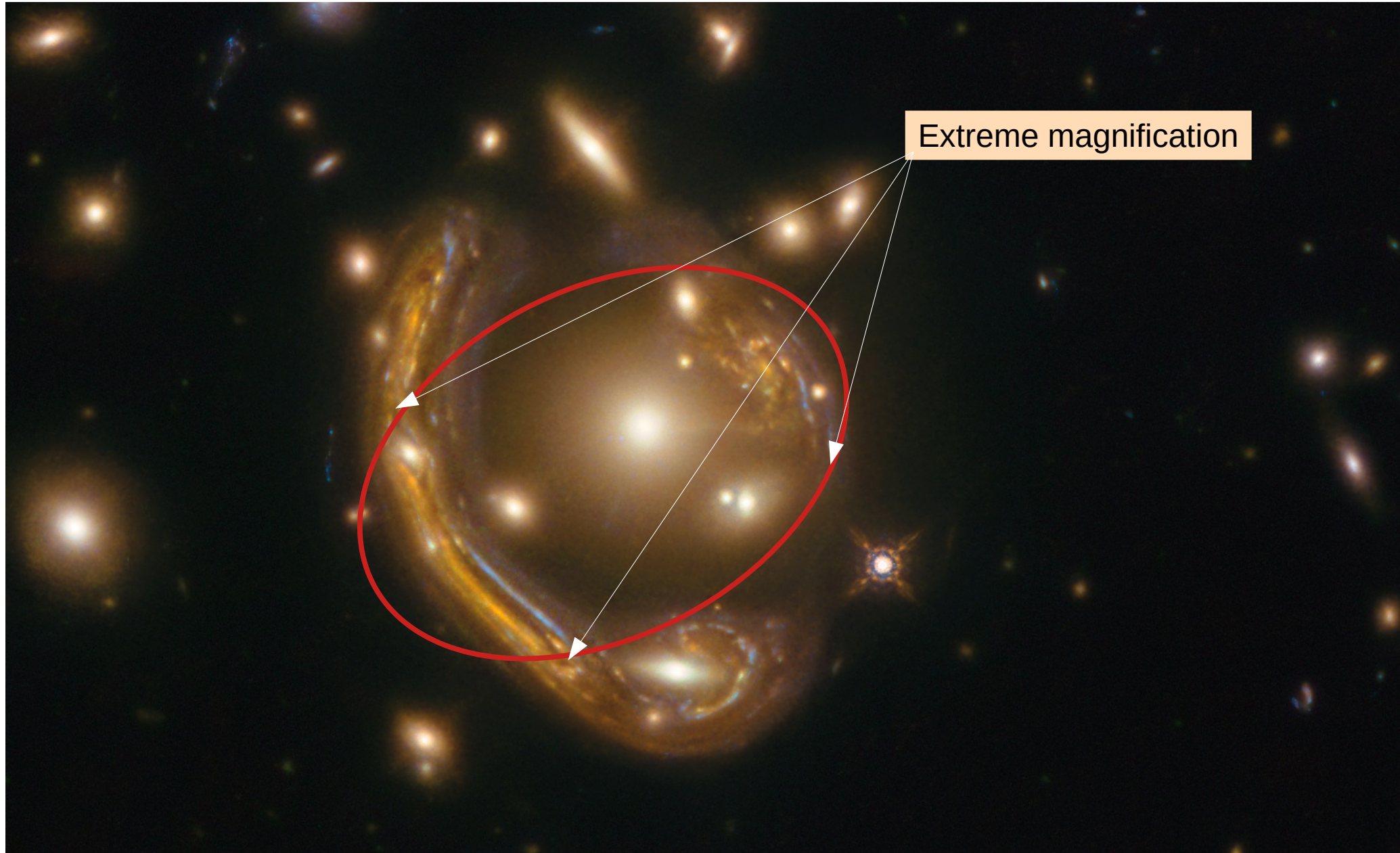
Strong Gravitational Lensing



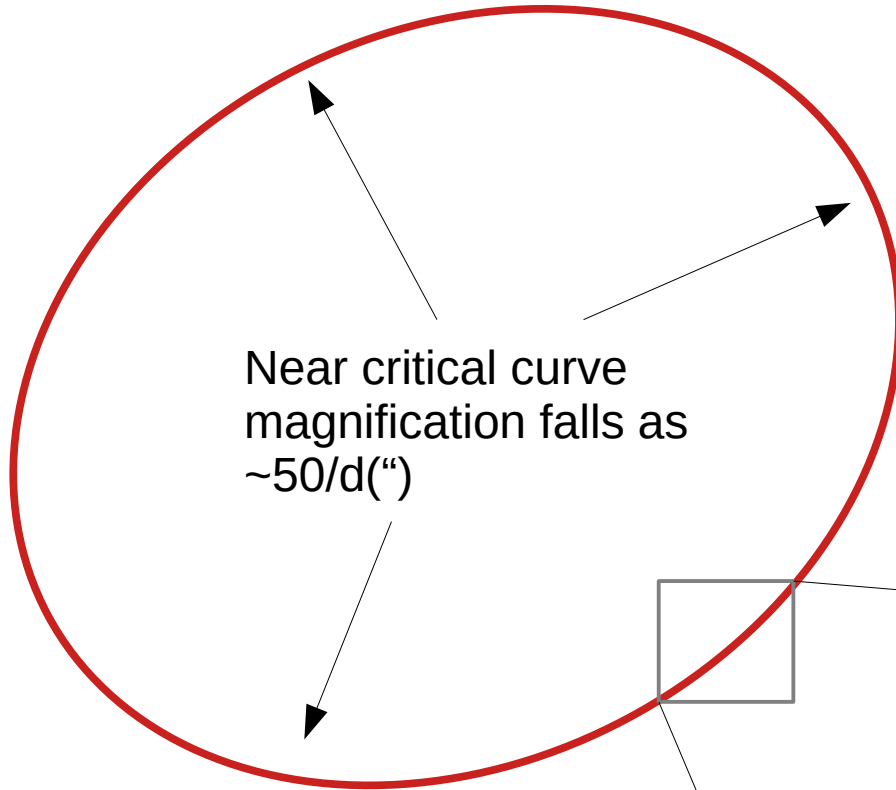
Strong Gravitational Lensing



Strong Gravitational Lensing

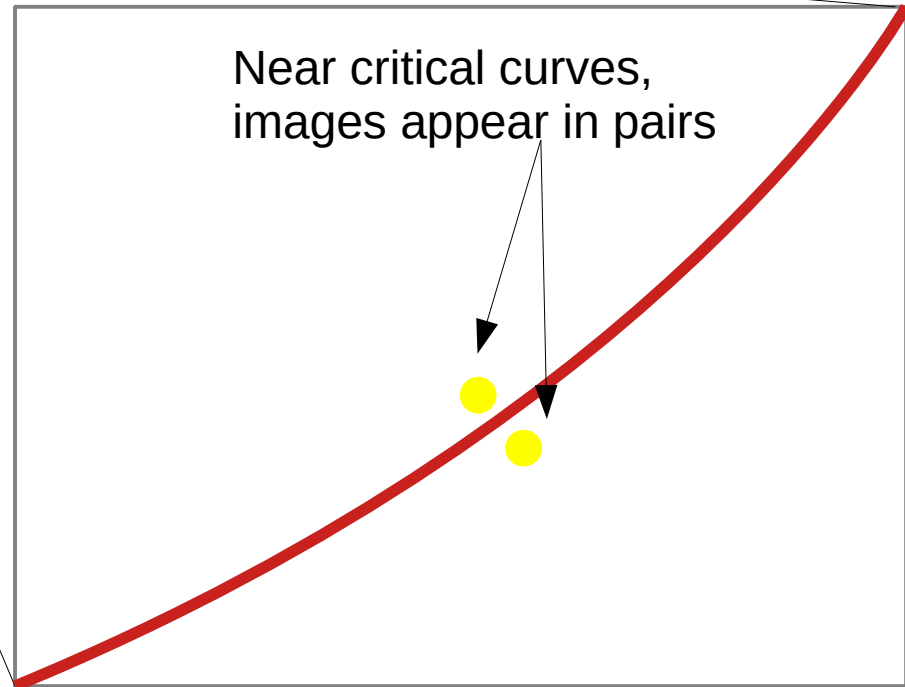
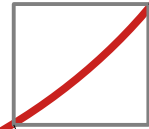


Gravitational lensing near critical curves

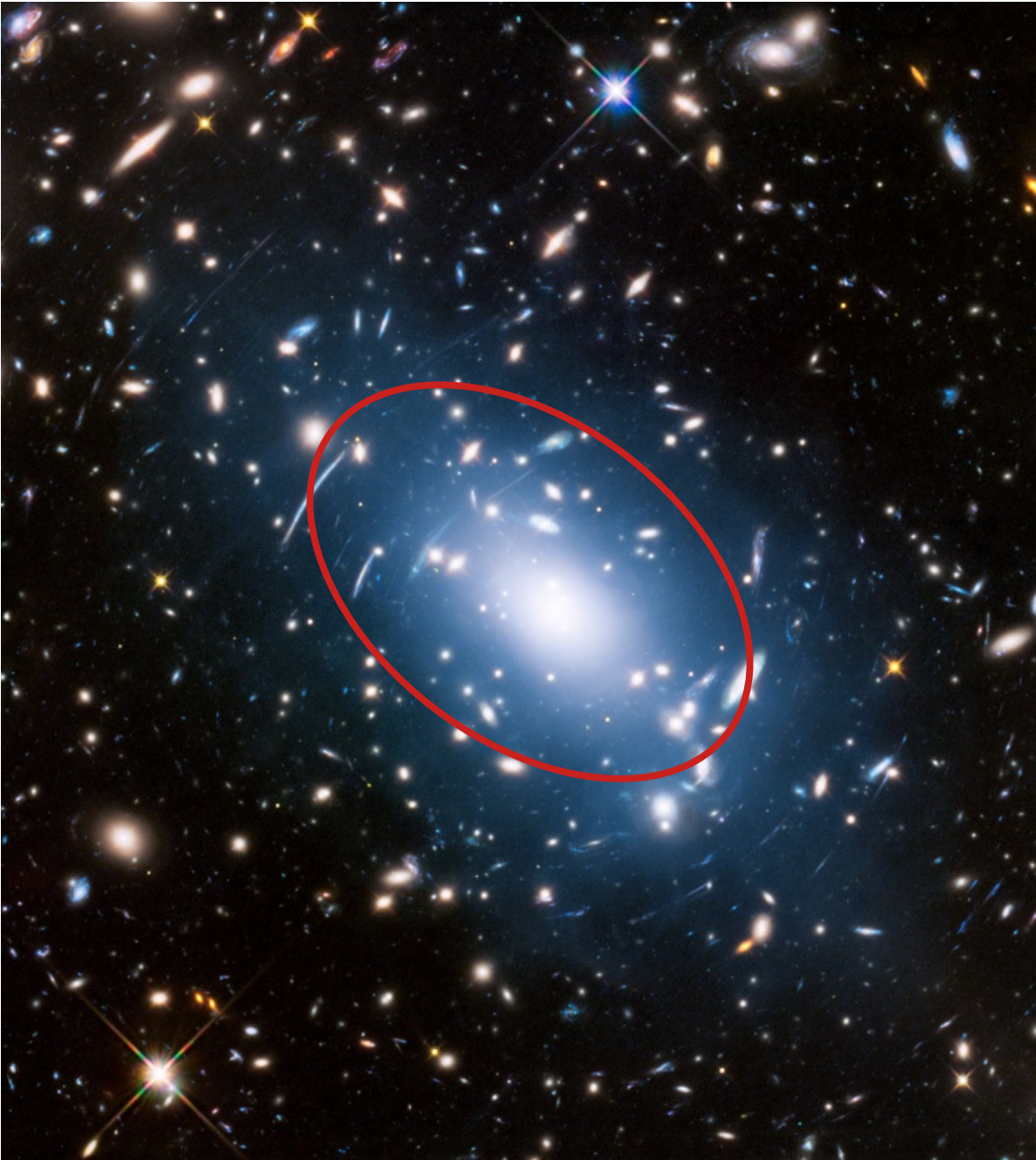


Magnification near the critical curve can reach thousands!

With microlenses, sometimes one of the images is hidden, specially for negative parity. Maximum magnification is lower.



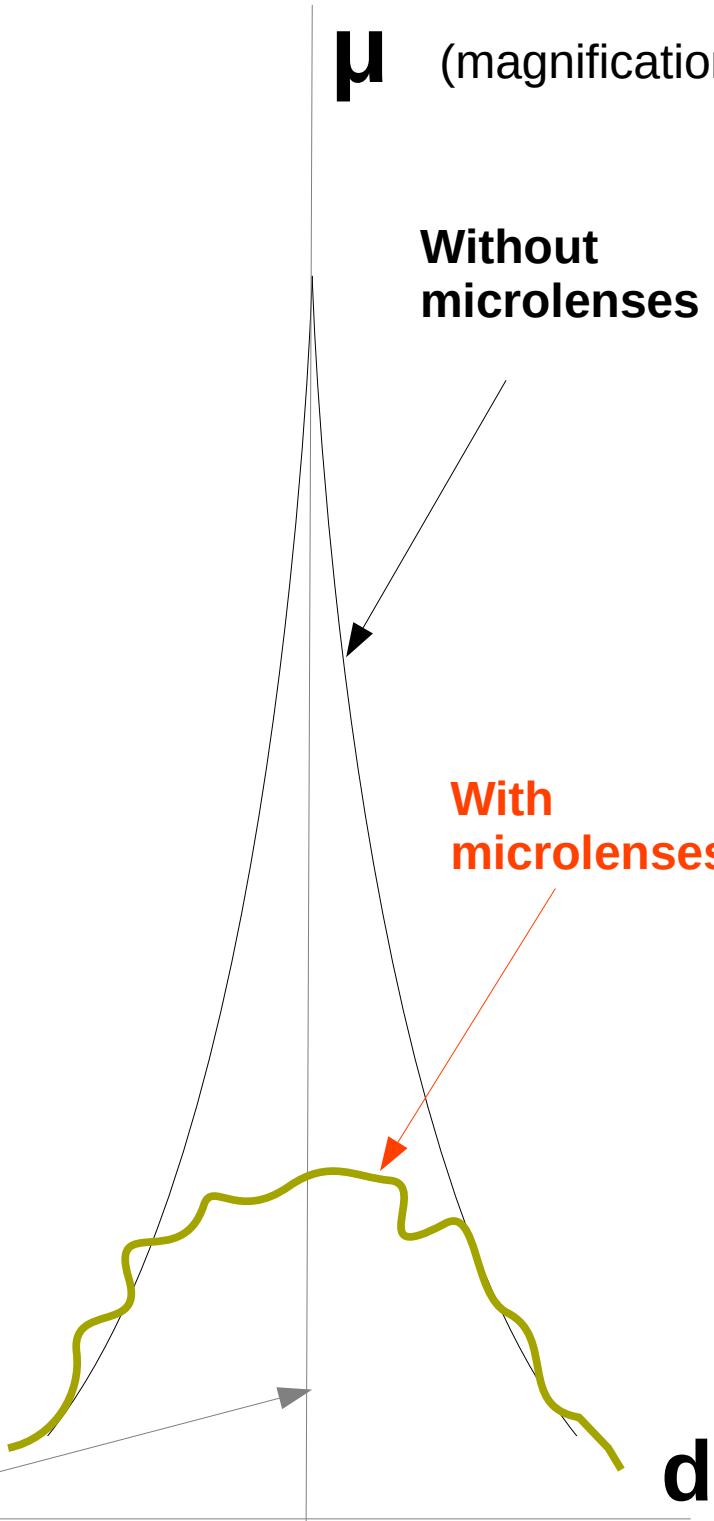
Microlenses distort the magnification



μ (magnification)

Without microlenses

With microlenses

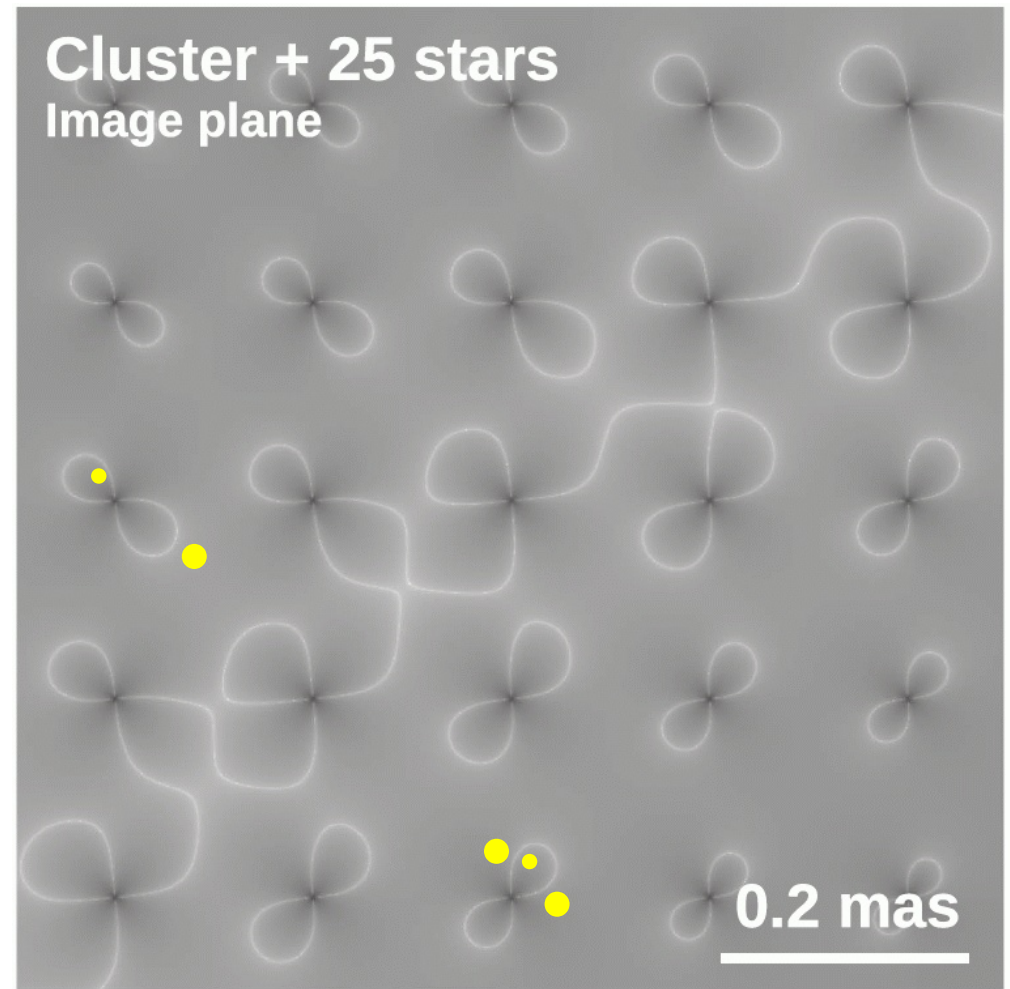
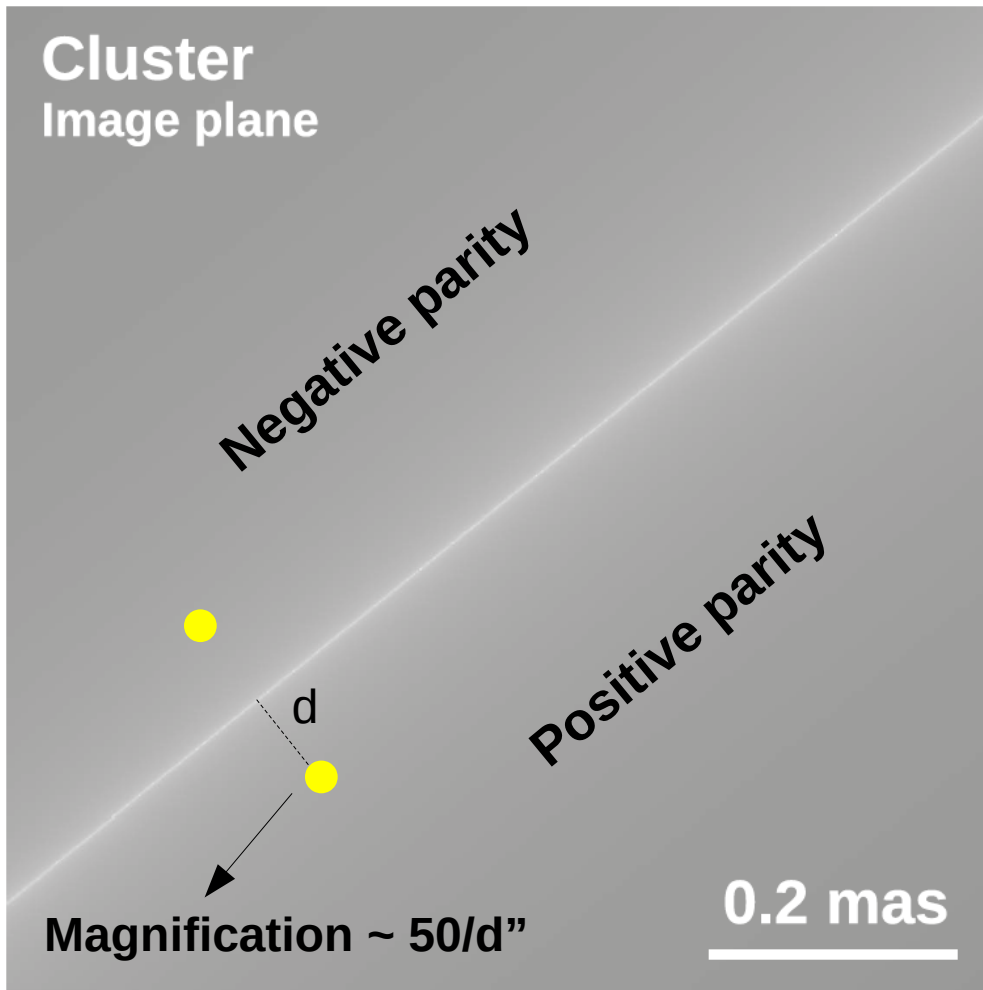


Critical Curve

Microlenses near Critical Curves

Microlenses with mass M near a caustic behave as having an effective mass $M^*\mu$.

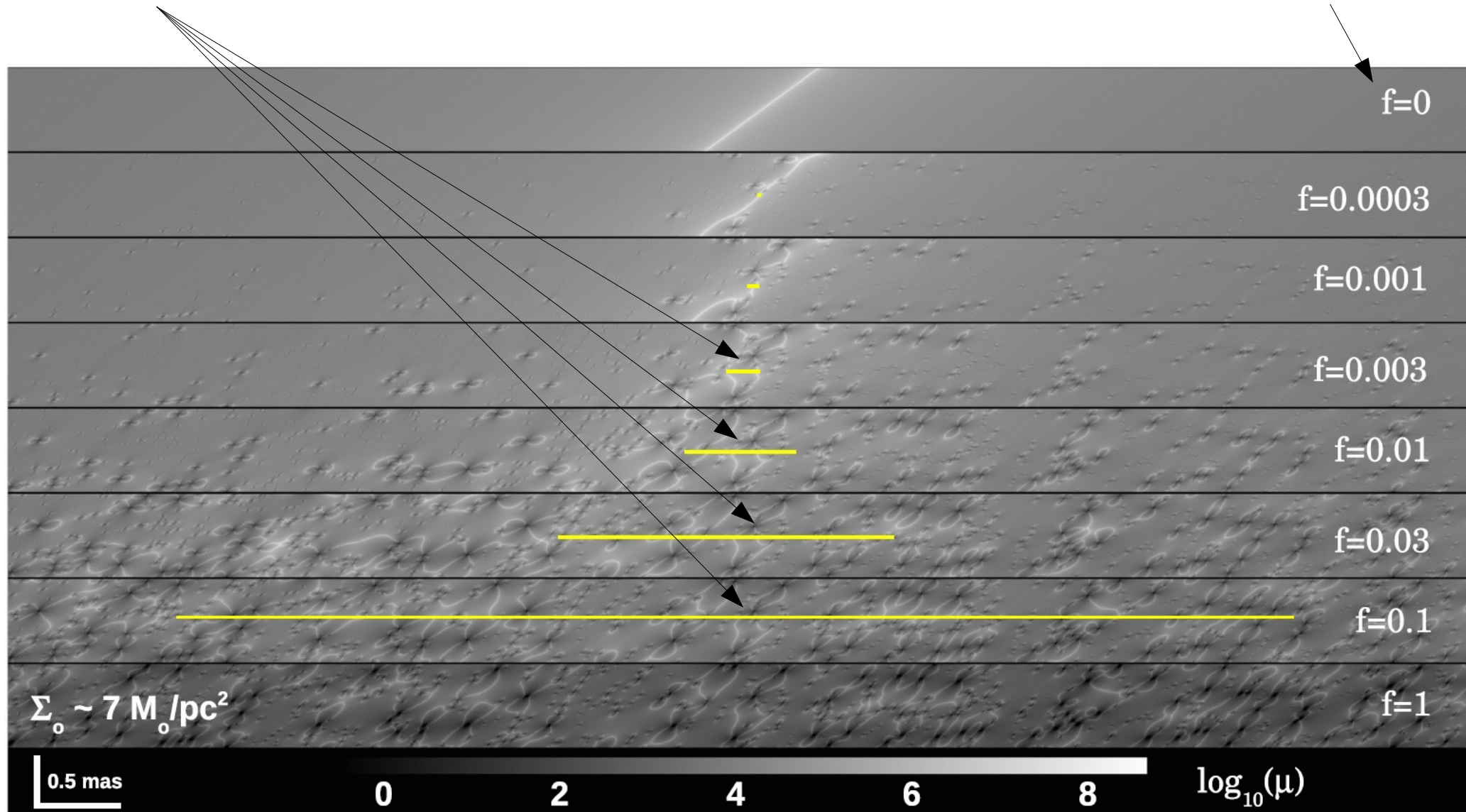
Microlenses behave very different depending on the sign of the magnification



Microlenses near Critical Curves

Width of saturation region proportional to $\mu \star \Sigma$

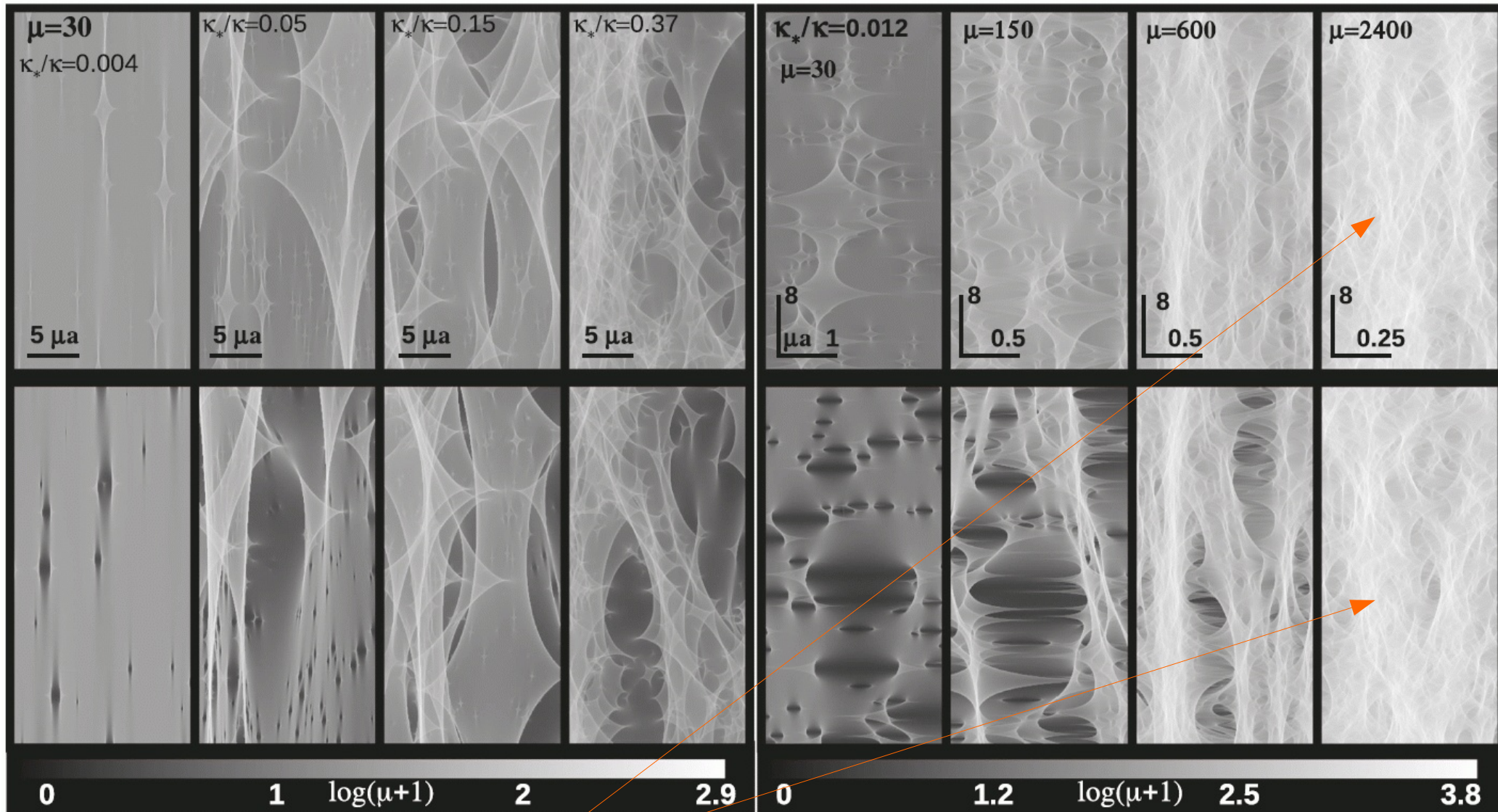
$$f = \Sigma / \Sigma_0$$



Microlenses near Critical Curves

Constant magnification

Constant surface mass density



Saturation regime

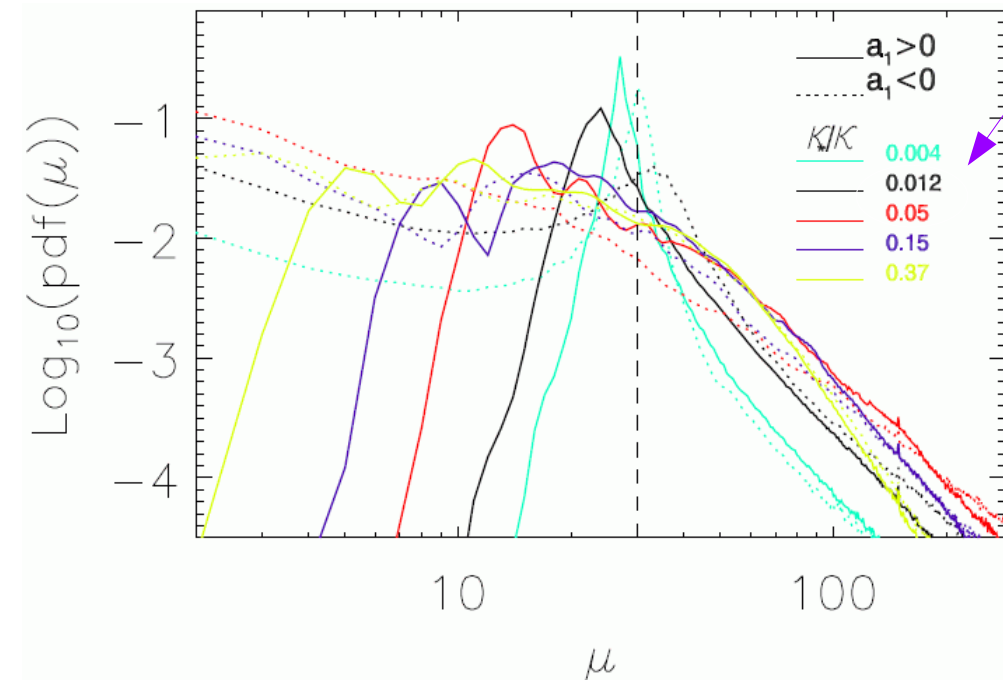
Statistics of Magnification

At “modest” magnifications, low surface mass densities (Σ) show largest asymmetry between negative and positive parity sides.
 $\Sigma \sim 0.05-0.1$ optimal for large flux fluctuations (can constraint PBH)

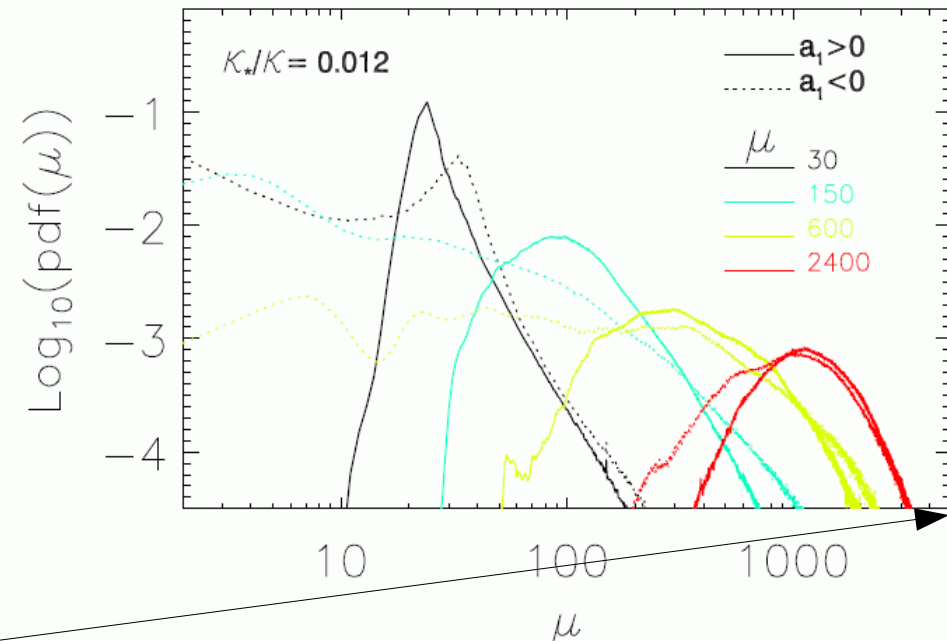
At large magnifications or κ_* , the pattern saturates and there is no distinction between parities (can constraint PBH)

Typical values

Constant magnification



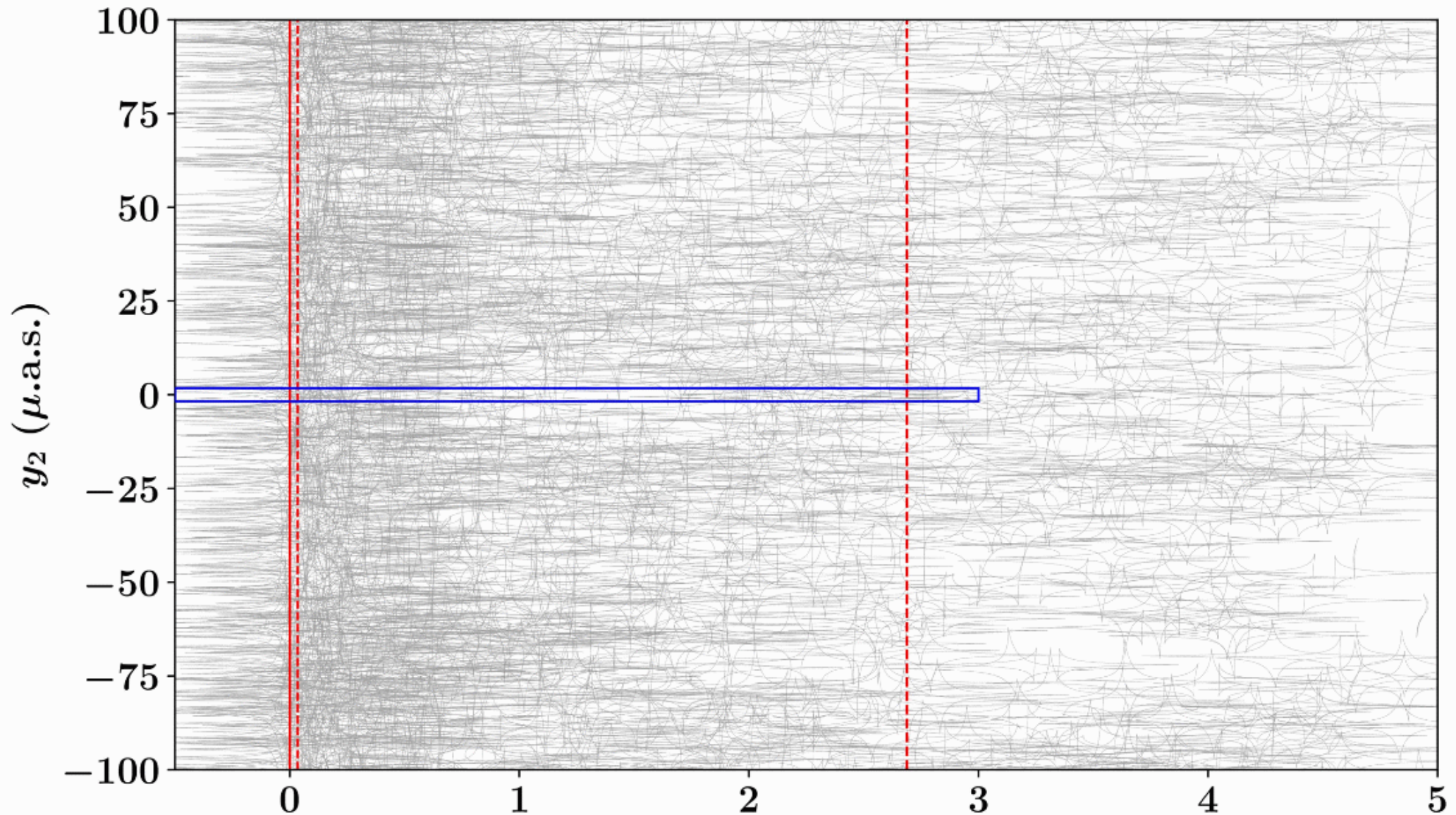
Constant surface mass density



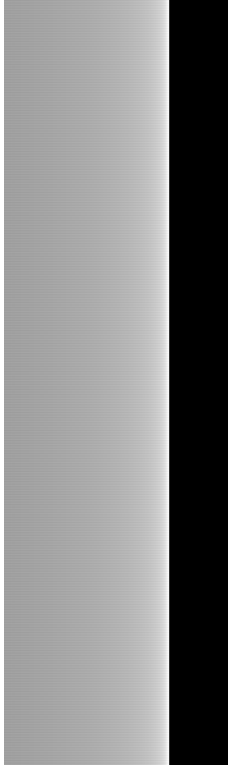
In the presence of microlenses, magnification factors larger than ~ 10000 are difficult

Diego, et al. 2018

Microcaustics form a network with increasing density as one approaches the critical curve.

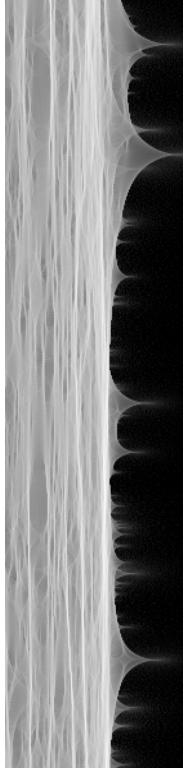


Smooth model

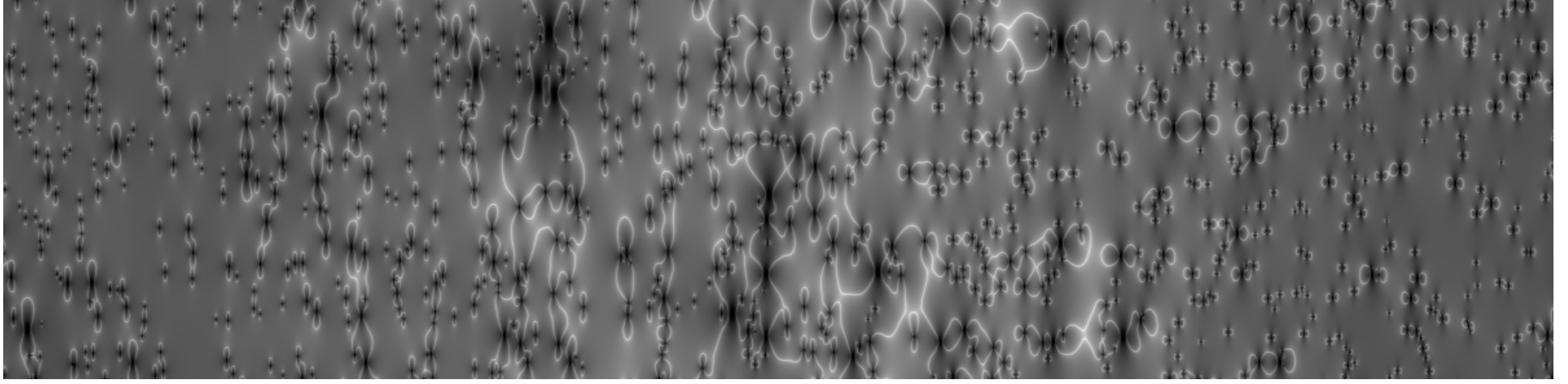
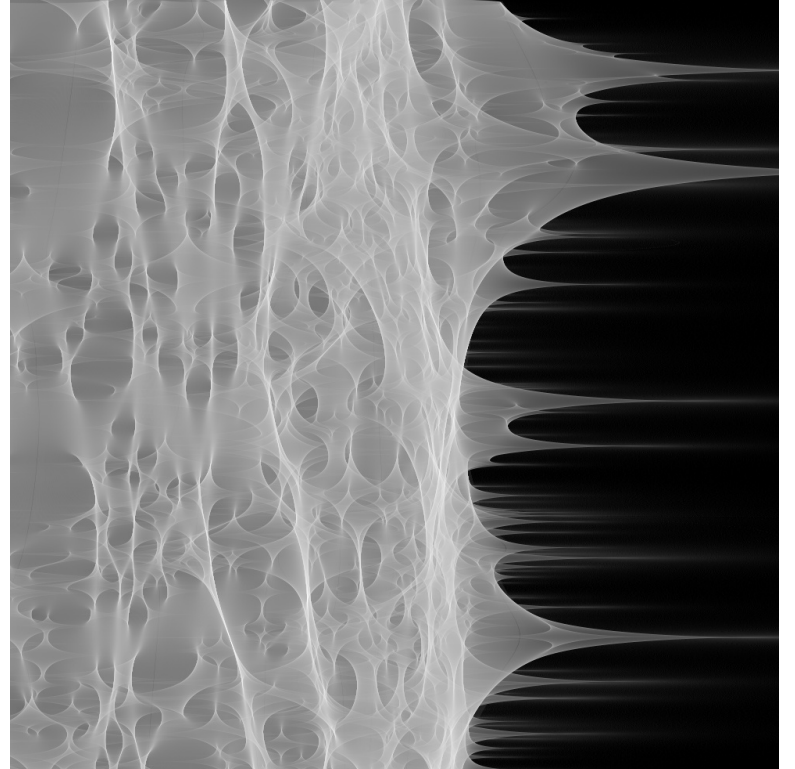


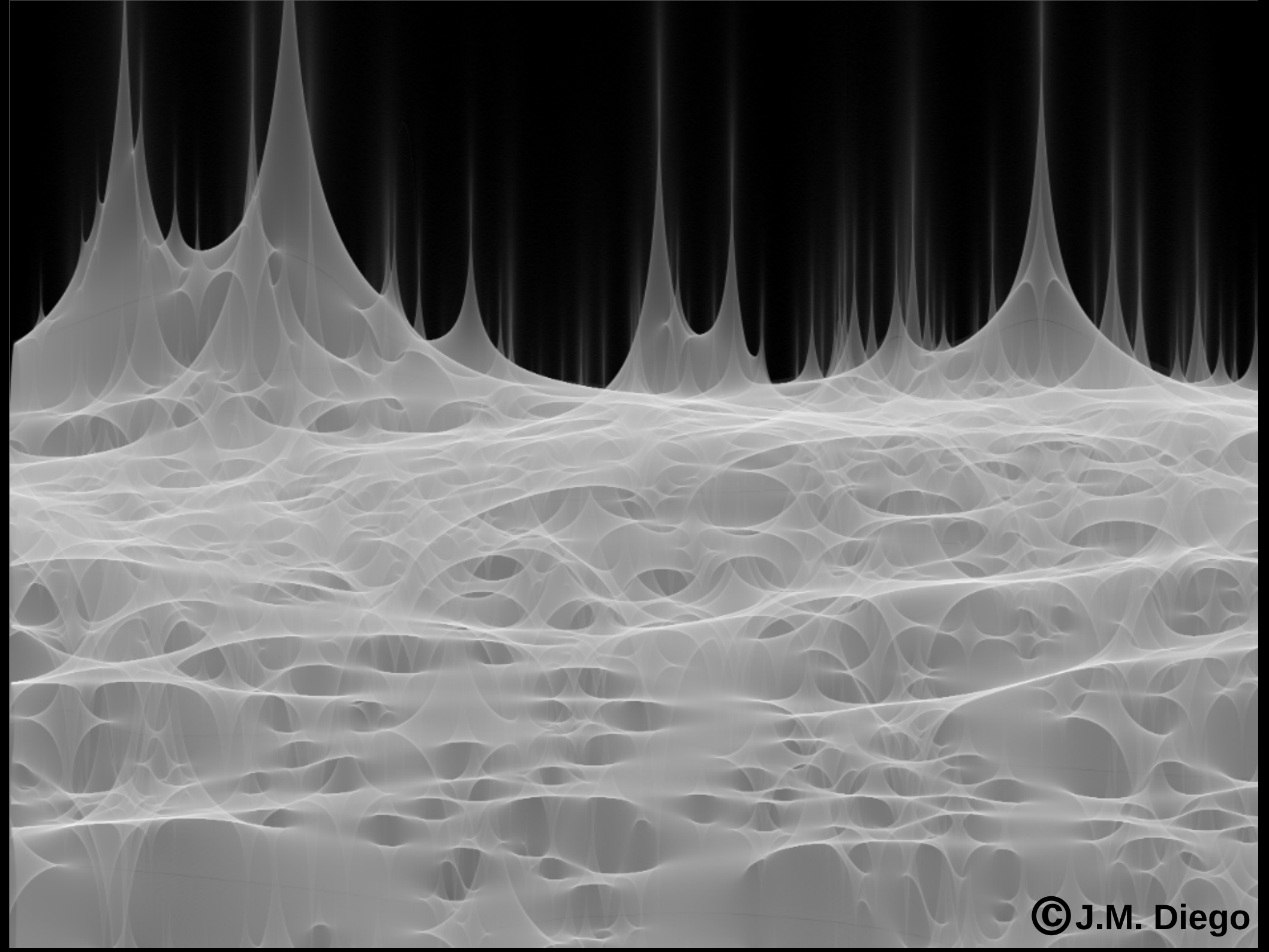
vs

Microlens model

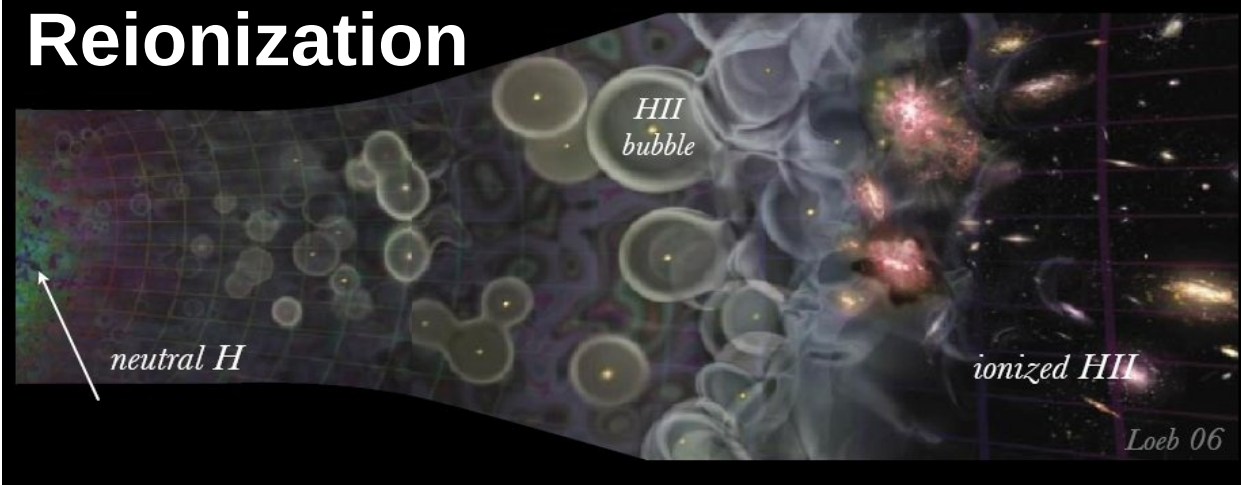


x10





Reionization



Pop II-III

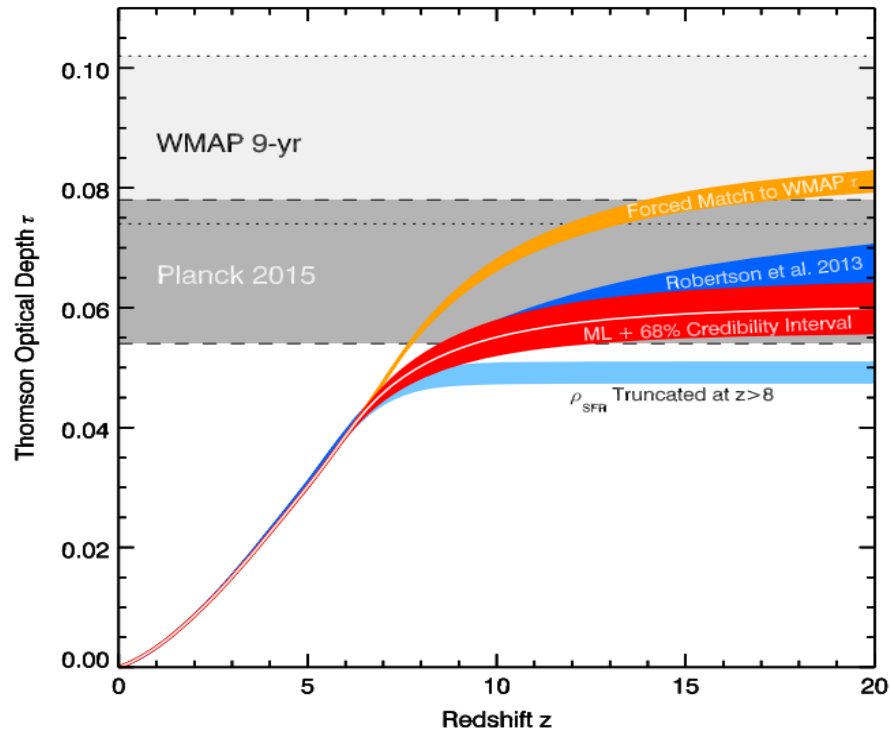
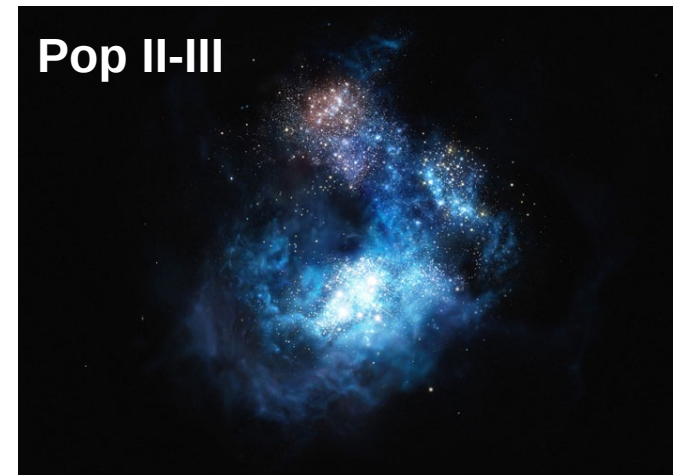
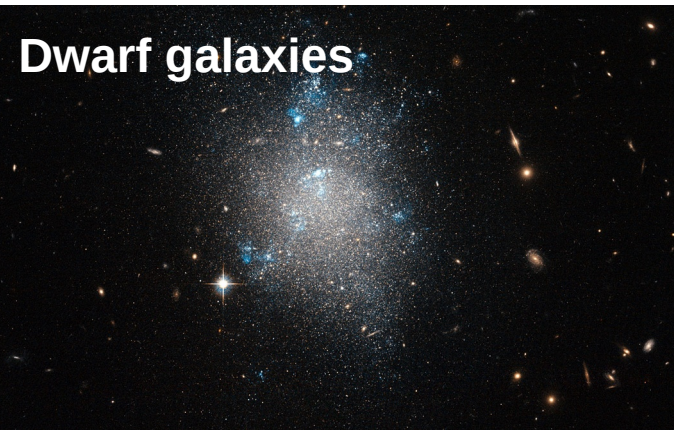
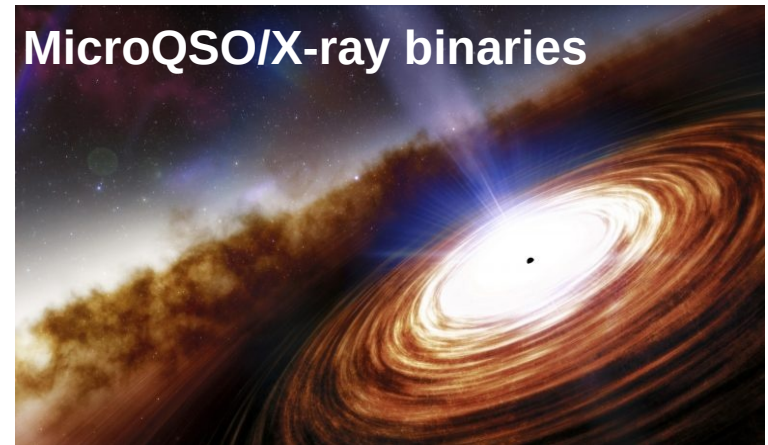
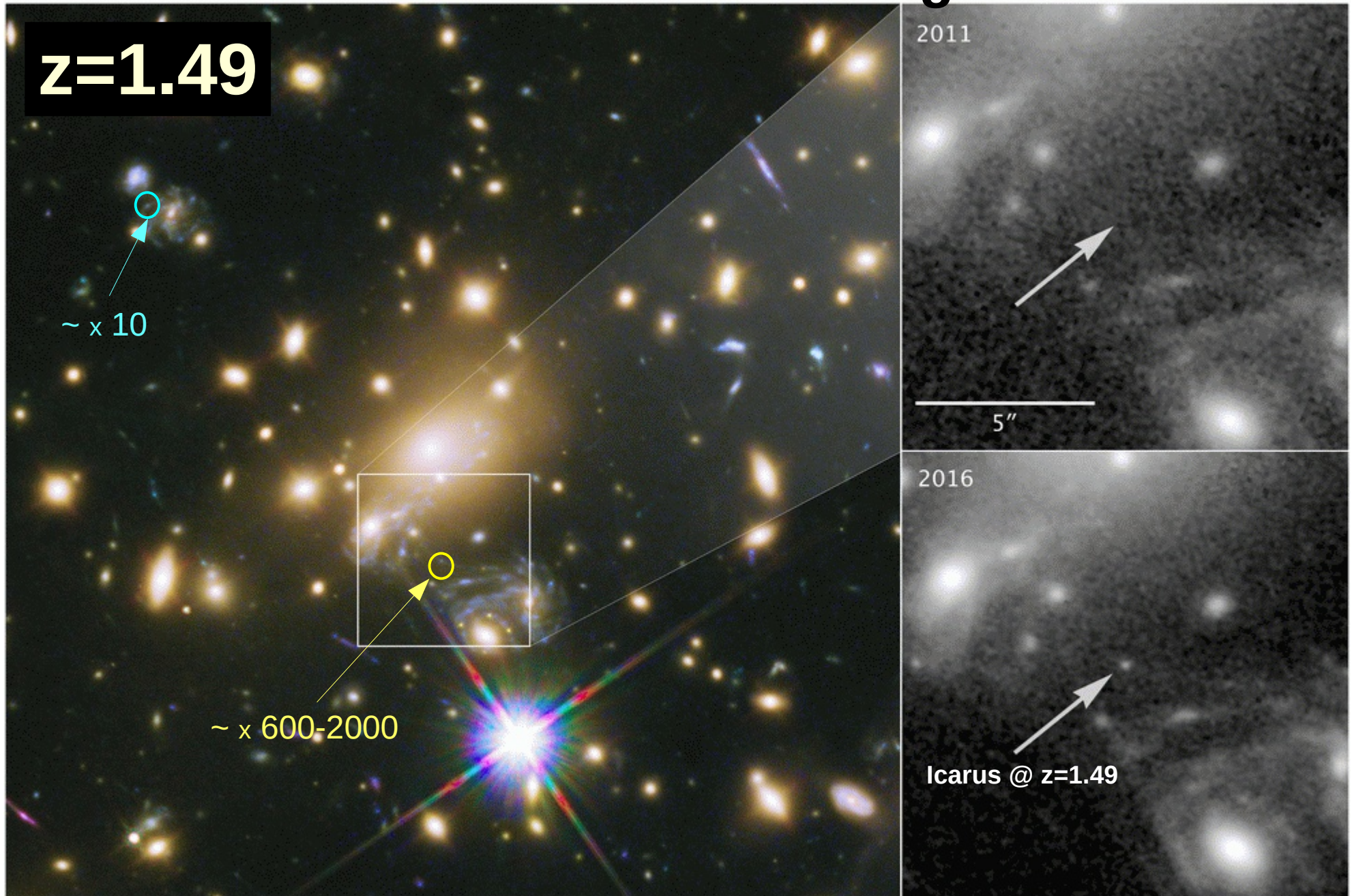


Figure 2. Thomson optical depth to electron scattering τ , integrated over redshift. Shown is the Planck constraint $\tau = 0.066 \pm 0.012$ (gray area), along with the marginalized 68% credibility interval (red region) computed from the SFR histories ρ_{SFR} shown in Figure 1. The corresponding inferences of $\tau(z)$ from Robertson et al. (2013; dark blue region), a model forced to reproduce the 9 yr WMAP τ constraints (orange region), and a model with ρ_{SFR} truncated at $z > 8$ (light blue region) following Oesch et al. (2014) are shown for comparison.

Robertson et al. 2015



Icarus. The First star at cosmological distance



MOTIVATION

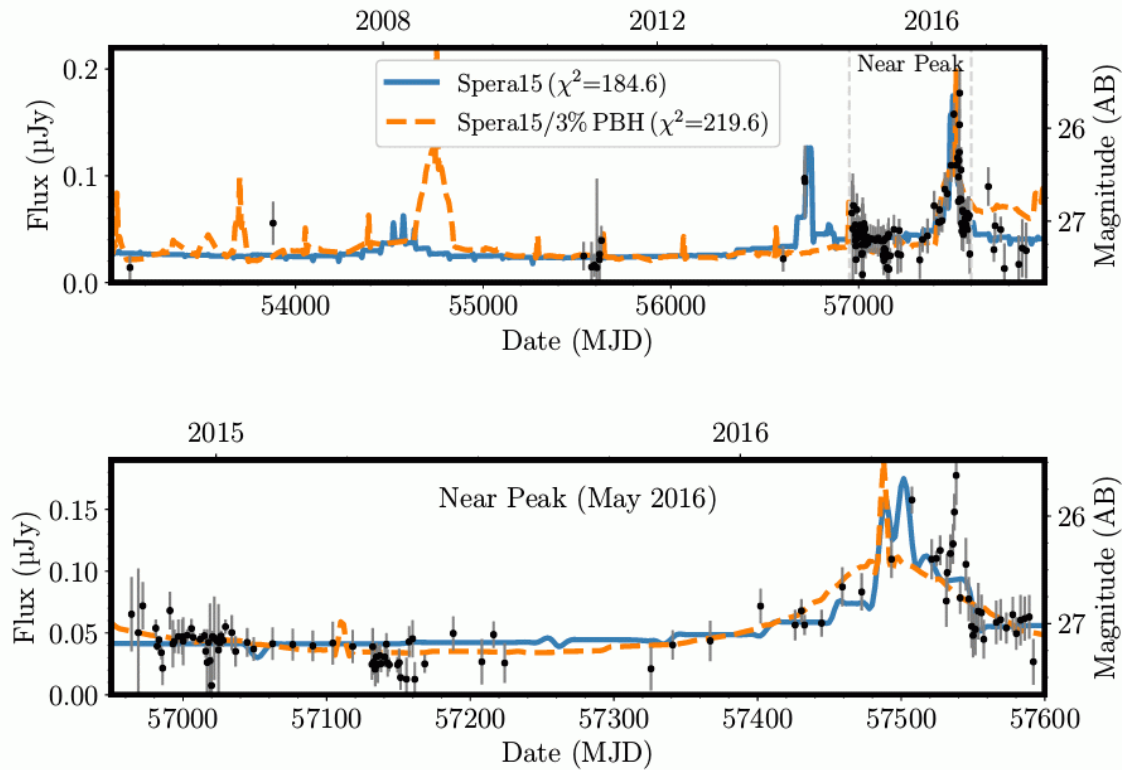
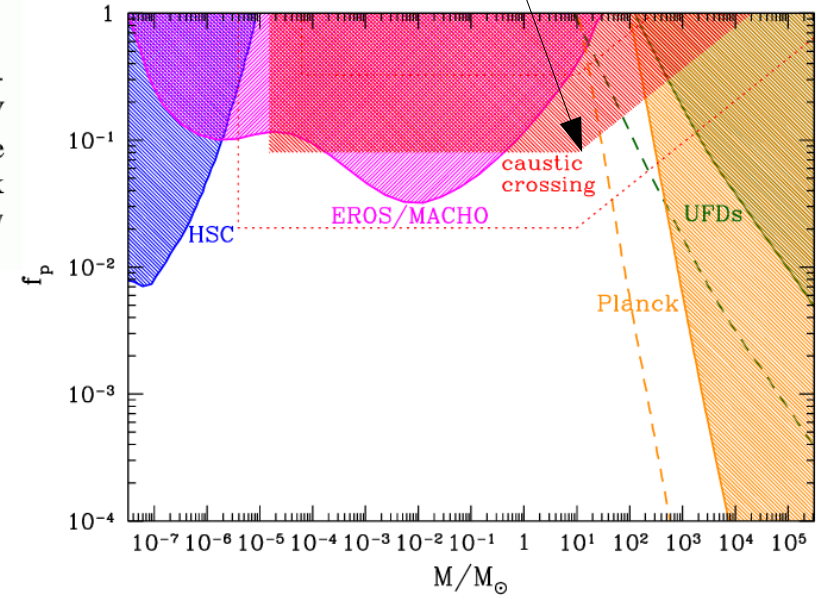


Figure 4: Light curve of the magnified star LS1, and best-matching simulated light curves during each interval. Fluxes measured through all wide-band *HST* filters are converted to F_{125W} using LS1's SED. The upper panel shows LS1's full *HST* light curve which begins in 2004. The lower panel shows the most densely sampled part of the light curve including the May 2016 peak (Lev16A). This maximum shows two successive peaks that may correspond to a lensed binary system of stars at $z = 1.49$.

Kelly, Diego et al 2018

Constraints on abundance of compact dark matter

Oguri, Diego et al 2018



First ever SED fit to a single star at $z > 1$

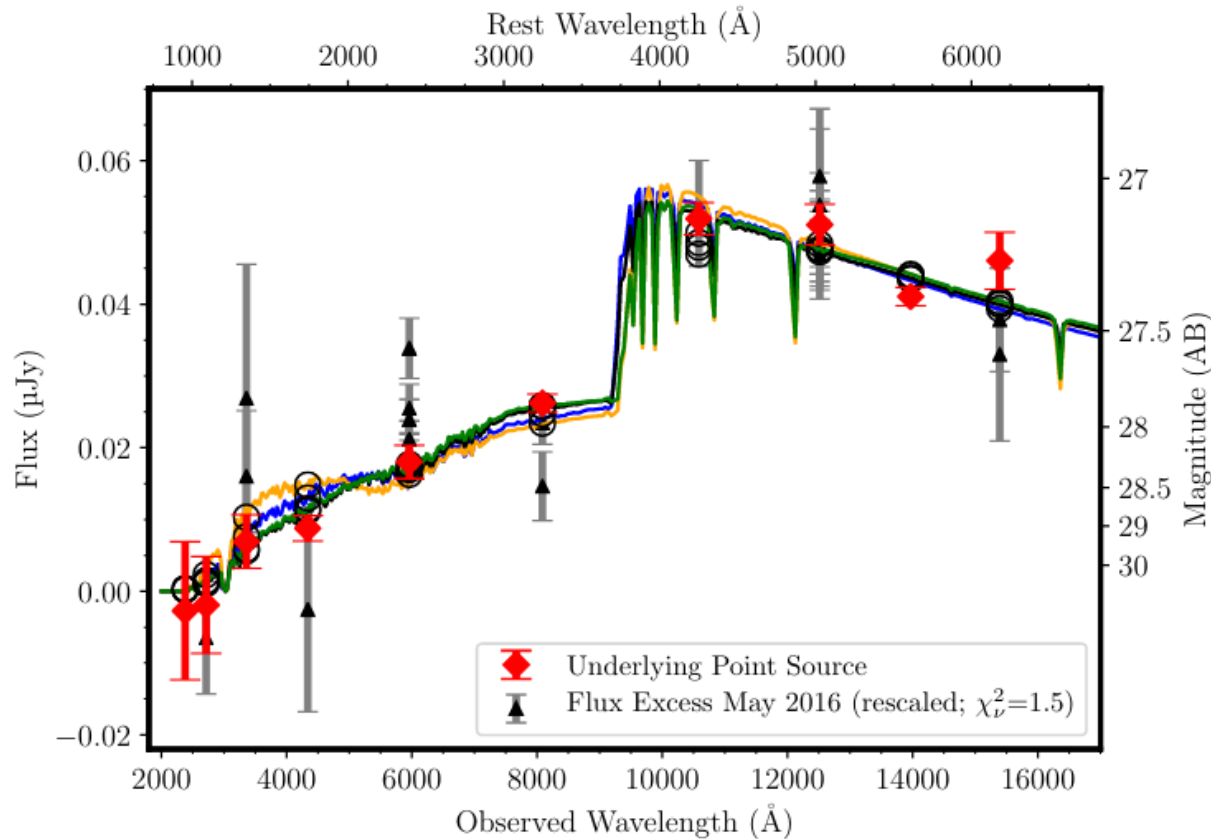


Figure 3: The SEDs of LS1 measured in 2013–2015 (red) and of the rescaled, excess flux density at LS1’s position close to its May 2016 peak (Lev16A; black) are consistent. Rescaling the SED of the flux excess to match to that of the 2013–2015 source yields $\chi^2_{\nu} = 1.5$, indicating that they are statistically consistent with each other despite a flux density difference of a factor of ~ 4 . The SED shows a strong Balmer break consistent with the host-galaxy redshift of 1.49, and stellar atmosphere models^[7] of a mid-to-late B-type star provide a reasonable fit. The blue curve has $T = 11,180$ K, $\log g = 2$, $A_V = 0.02$, and $\chi^2 = 16.3$; the orange curve has $T = 12,250$ K, $\log g = 4$, $A_V = 0.08$, and $\chi^2 = 30.6$; the black curve has $T = 12,375$ K, $\log g = 2$, $A_V = 0.08$, and $\chi^2 = 12.9$; and the green curve has $T = 13,591$ K, $\log g = 4$, $A_V = 0.13$, and $\chi^2 = 16.5$. Black circles show the expected flux density for each model.

Godzilla. A Monster star at $z=2.37$

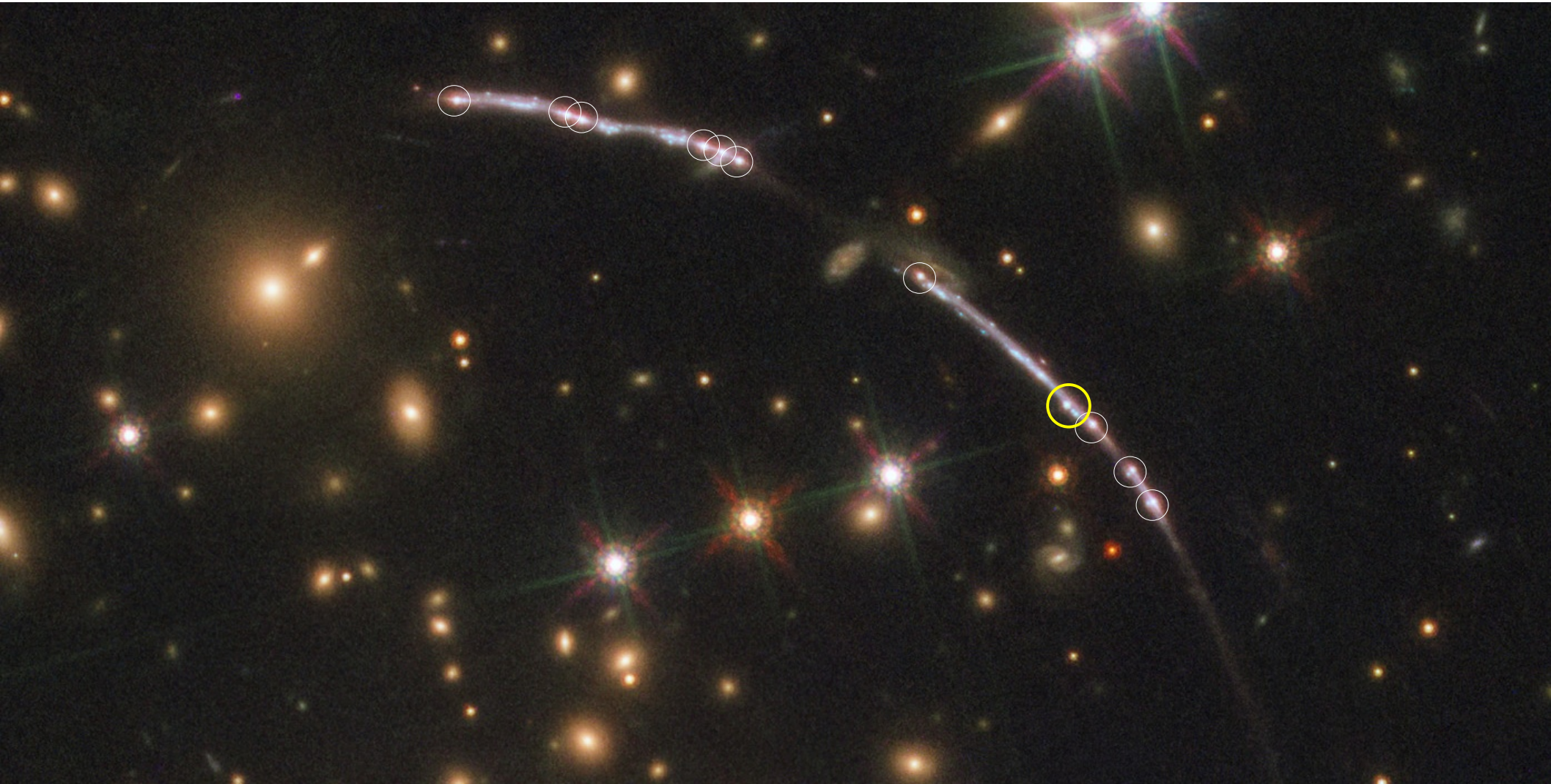
$Z=2.37$

MUSE FoV



Diego et al. 2022

Godzilla. A Monster star at $z=2.37$



Multiple images of the same stellar cluster (white circles)

Godzilla is seen only once (yellow circle) which is unexpected (should be seen multiple times)

Godzilla is unresolved

Godzilla. A Monster star at $z=2.37$

Lack of counterimages and unresolved nature

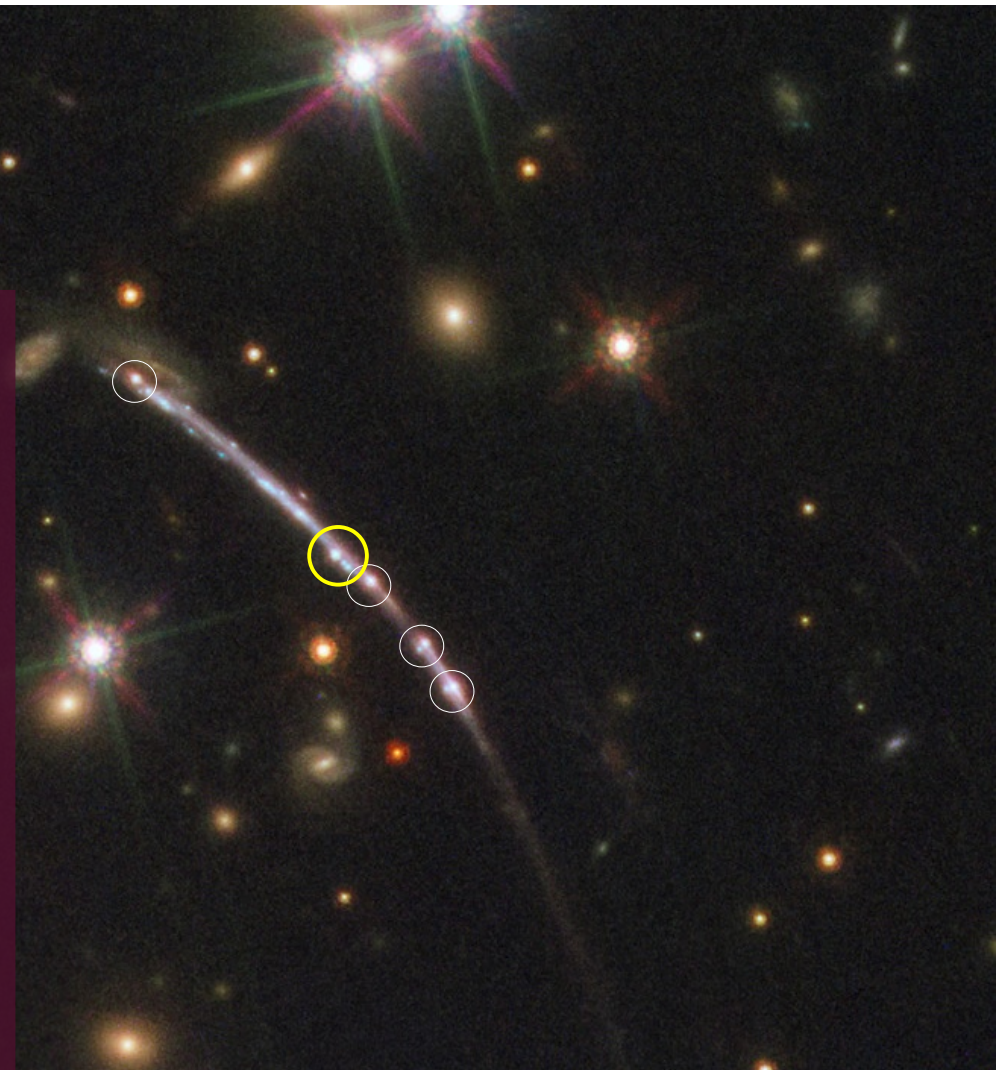
Globular Cluster? \longrightarrow No

SN & time delays? \longrightarrow No

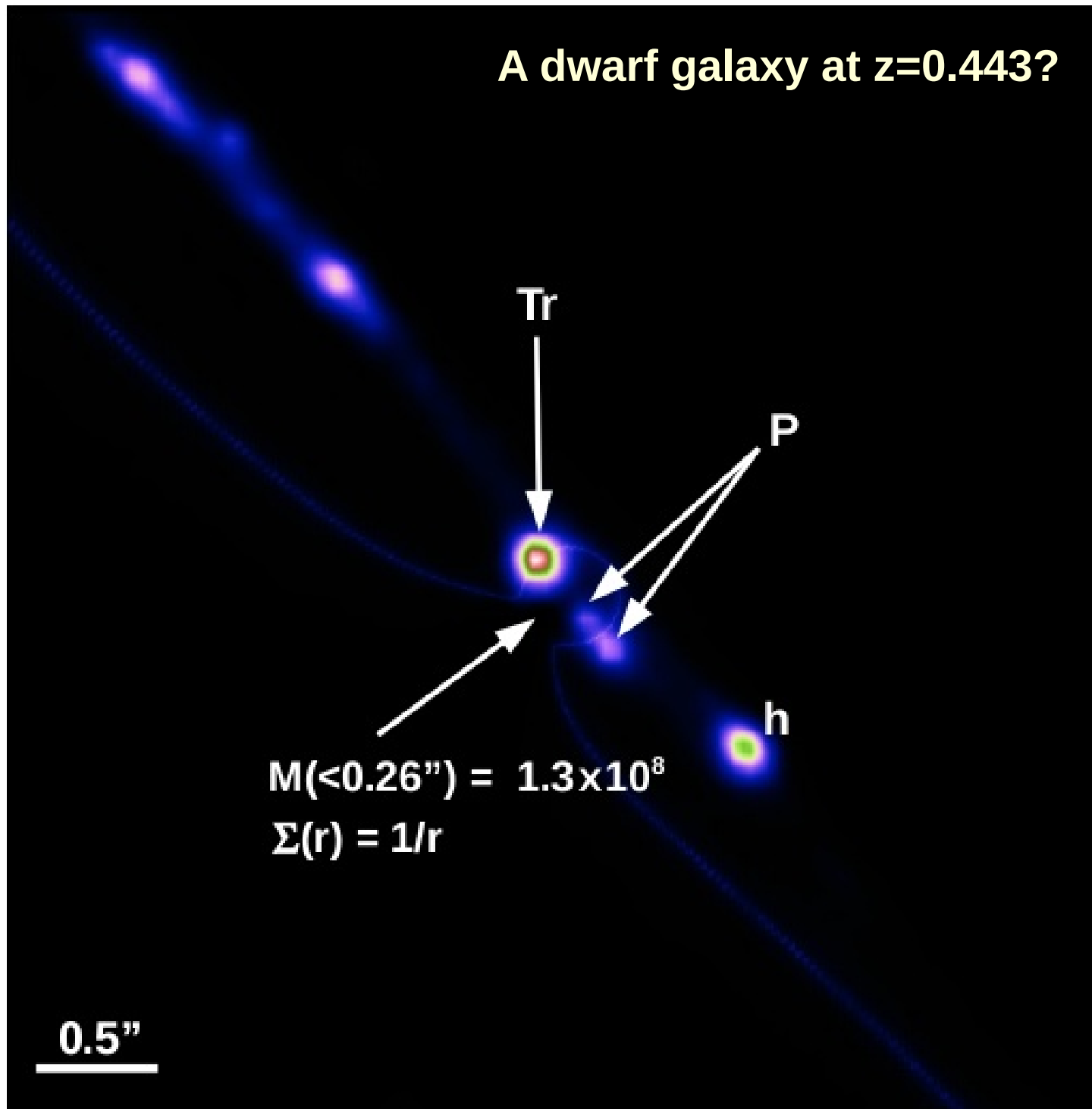
Extreme magnification? \longrightarrow Yes

$R < 0.3$ pc \longleftarrow Magnification ~ 5000

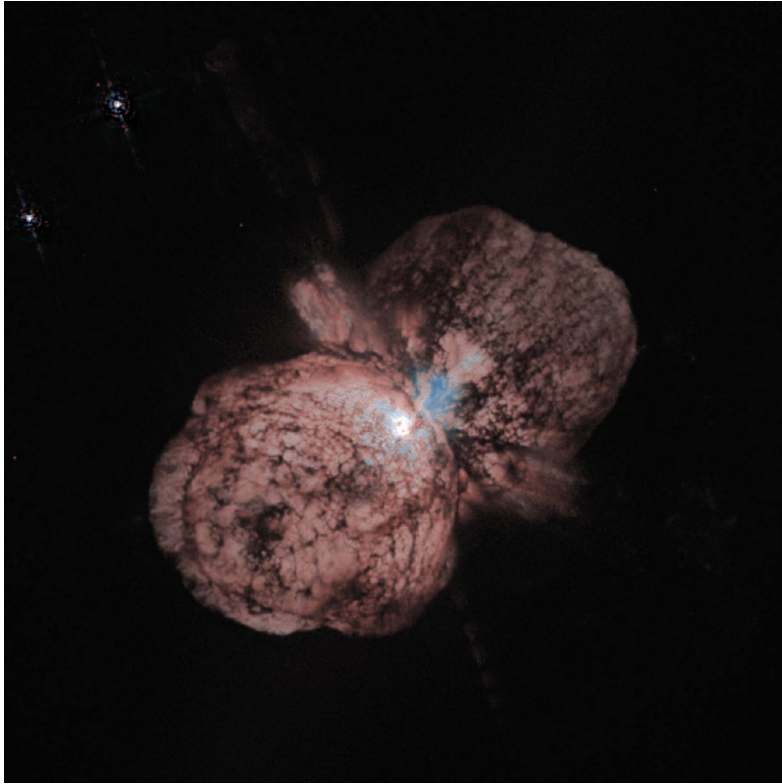
Monster Star? \longleftarrow Magnitude ~ -15



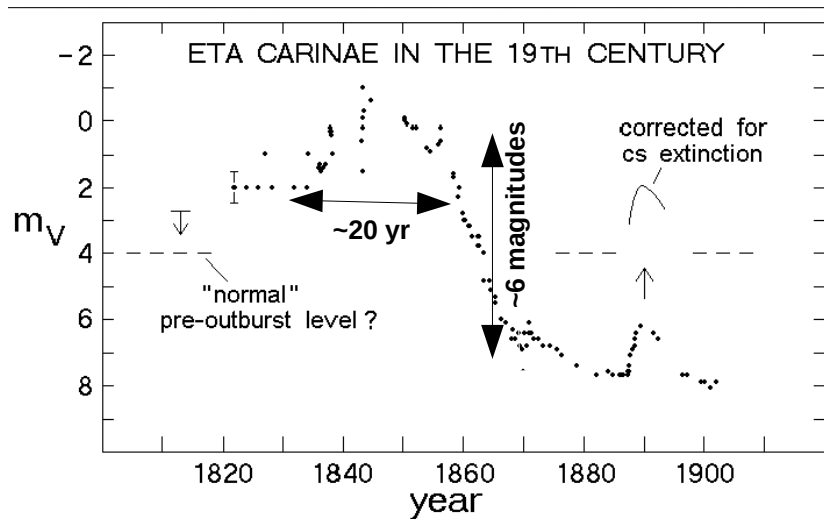
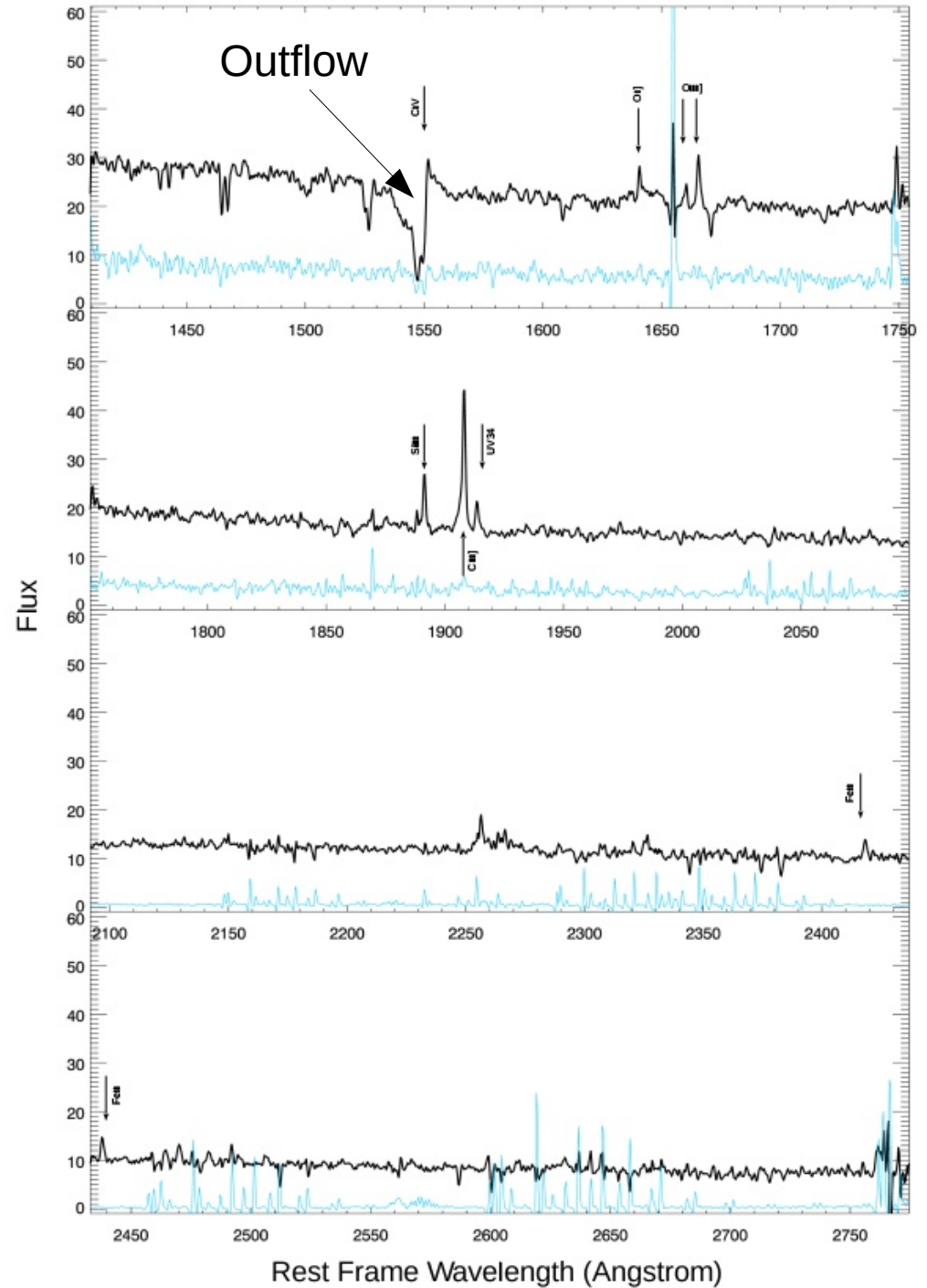
A dwarf galaxy at $z=0.443$?



MUSE spectrum of Godzilla

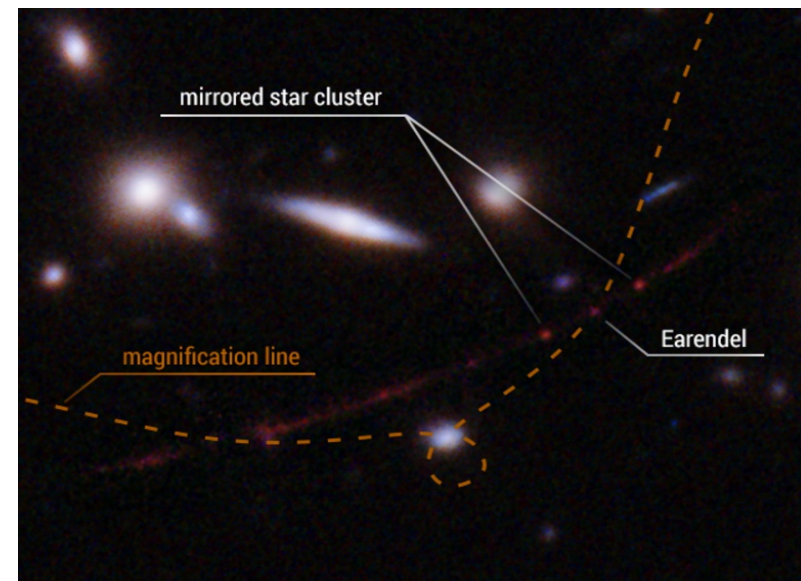


First ever spectrum of a single star at $z > 2$



Earendel. The farthest known star at $z=6.2$

$Z=6.2$



Multiple lens models predict maximum magnification around Earendel

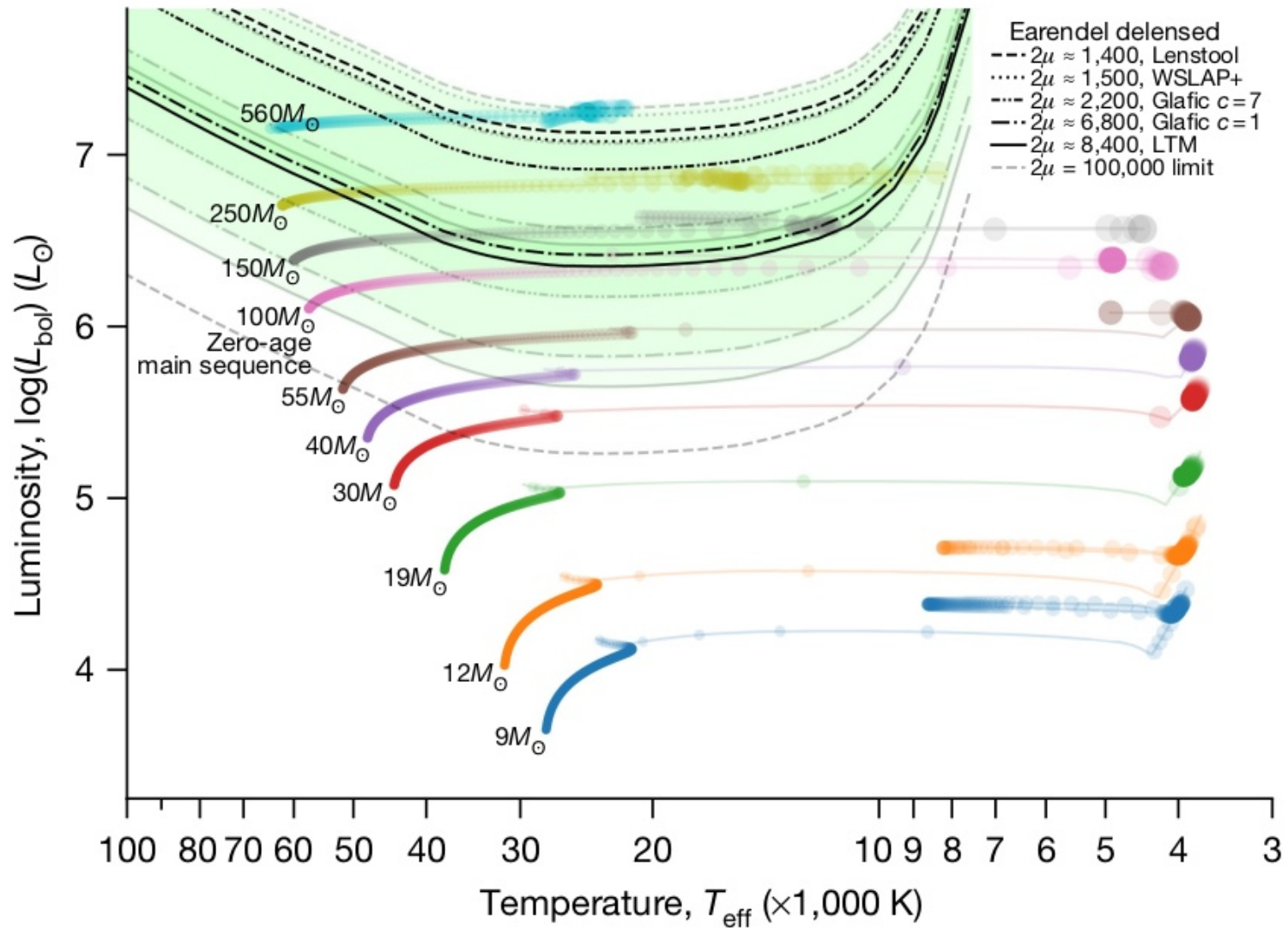
The fact that it is unresolved constrains the size to less than ~ 0.4 pc

Magnification can be in the range of thousands

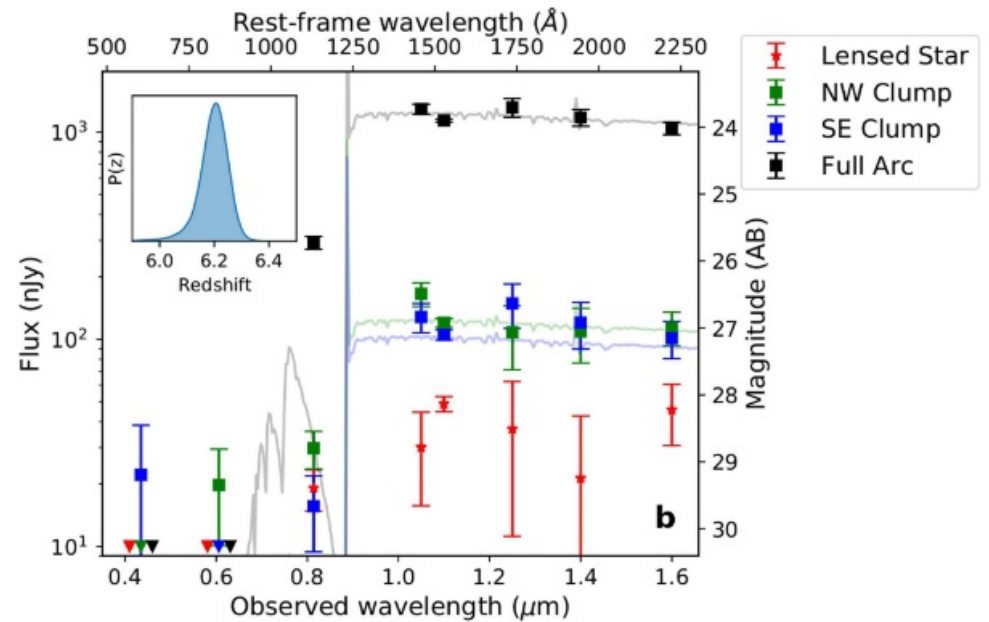
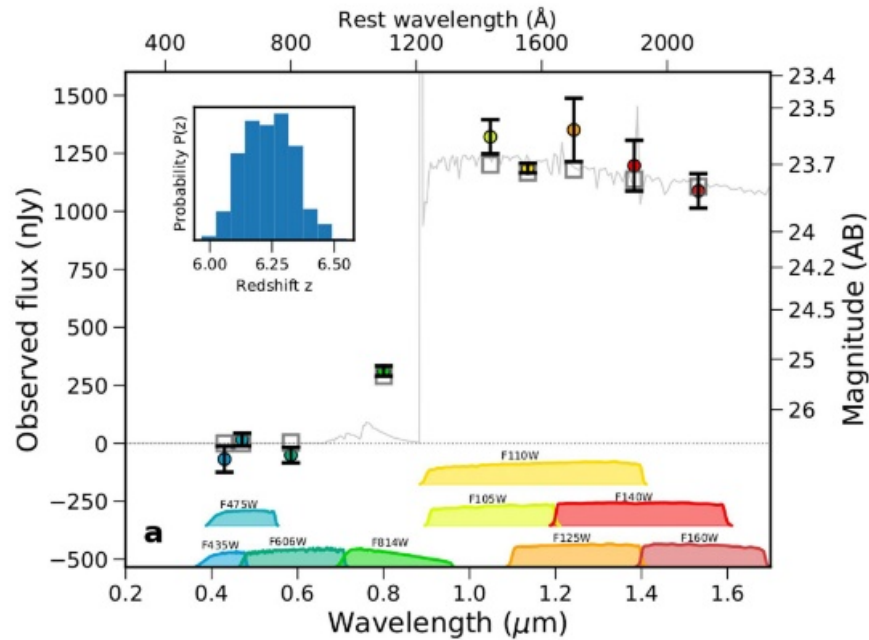
Lack of second image implies the pair of images must be forming an unresolved image. At this magnification hiding second image is not possible.

Welch, Coe, Diego et al. 2022

Earendel. The farthest known star at $z=6.2$



- Mass above $\sim 100 M_{\text{sun}}$ and temperature above 15K
- Need JWST to narrow down stellar parameters
- Star might disappear behind the caustic in ~ 10 years

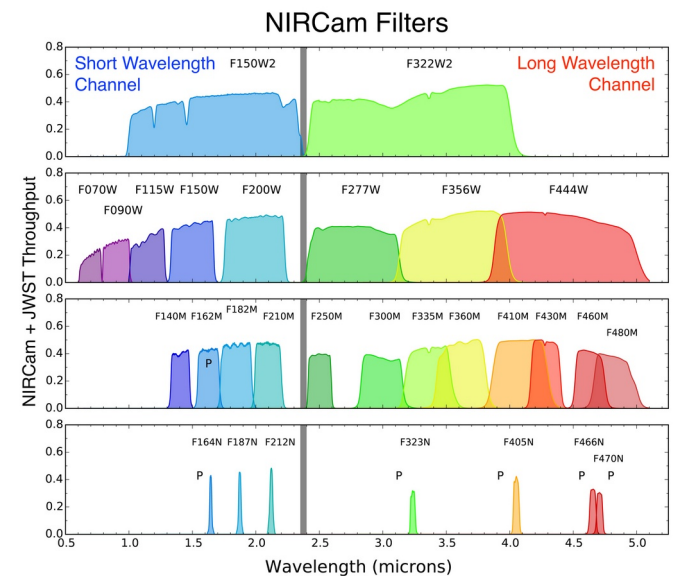


Extended Data Fig. 1 | Photometry of the Sunrise Arc and Earendel. a, HST photometry with 1σ error bars, SED fit, and redshift probability distribution for the Sunrise Arc using the photometric fitting code BAGPIPES. The arc shows a clear Lyman break feature, and has a photometric redshift $z = 6.24 \pm 0.10$ (68% CL). **b**, HST photometry for the full arc (black), clumps 1.1a/b (green/blue),

and Earendel (red), with associated 1σ error bars. BPZ yields a photometric redshift of $z_{\text{phot}} = 6.20 \pm 0.05$ (inset; 68% CL), similar to the BAGPIPES result. Clumps 1.1a/b have similar photometry, strengthening the conclusion that they are multiple images. Note both BPZ and BAGPIPES find significant likelihood only between $5.95 < z < 6.55$ for the Sunrise Arc.

First ever SED of a single star at $z > 6$

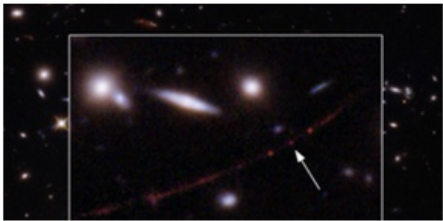
Need to wait for JWST for better data



How to measure the impact of your research



Bruce Willis deja Hollywood para empezar su carrera en España tras ser diagnosticado con una enfermedad que afecta al habla



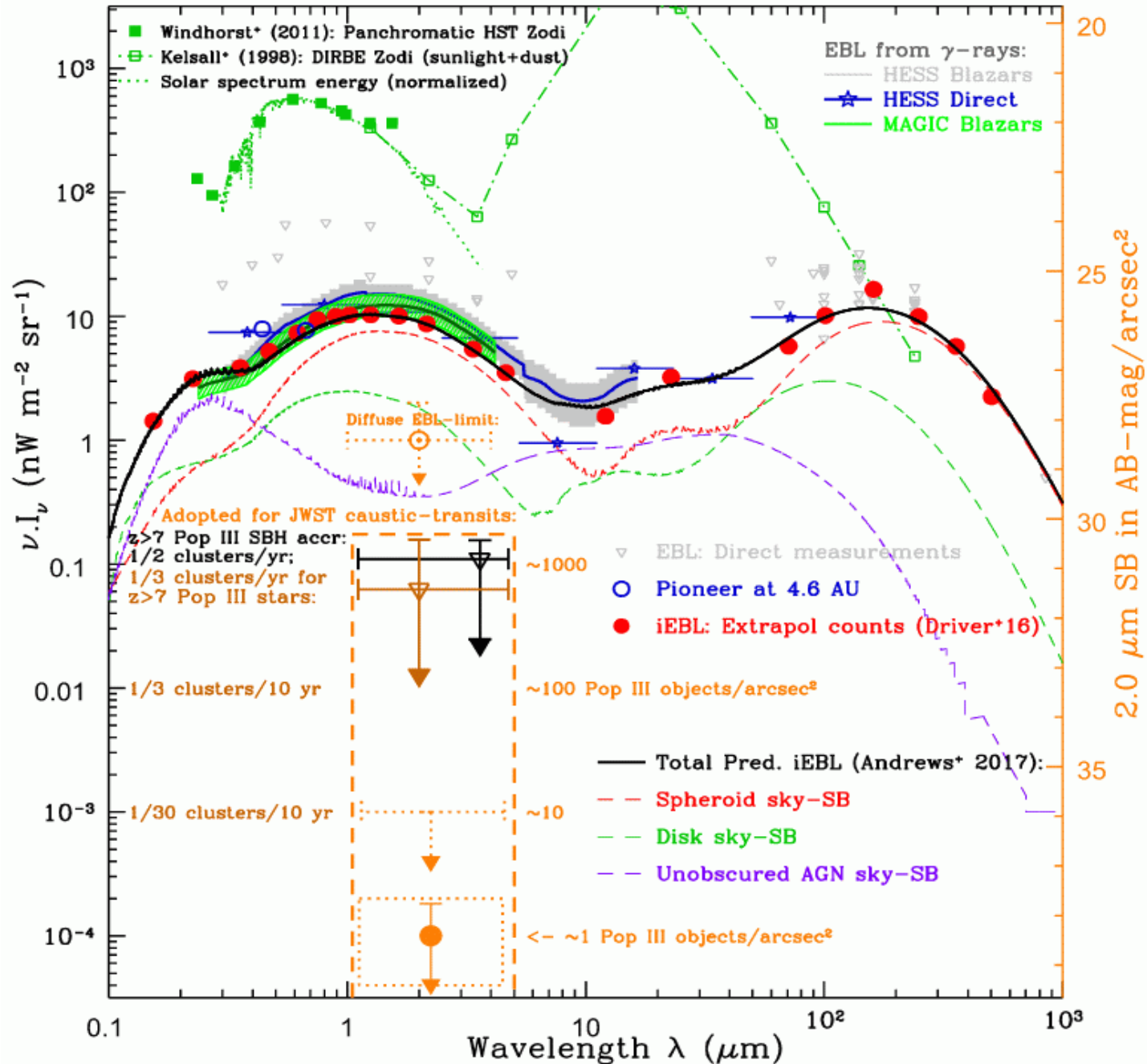
El telescopio «Hubble» descubre una estrella lejana en la que no se habla de la bofetada de Will Smith



Pedro Sánchez asegura que no eliminará la Filosofía, «sea lo que sea eso», de los planes de estudio

The "Hubble" telescope discovers a distant star in which there is no talk of Will Smith's slap

Detecting Pop III with JWST



CONCLUSIONS

Individual stars can be studied at $z > 6$ thanks to extreme magnification. Directly identify the sources of reionization.

Limitation on the maximum magnification from microlenses naturally imposes a selection effect toward the brightest stars.

These stars can be used as background beacons to constrain models of dark matter (primordial black holes, wave-dark matter).

JWST can potentially observe Pop III stars.

Other very compact sources are subject also to extreme magnification. For instance gravitational waves detected with LIGO-Virgo-KAGRA

Lensing and LIGO-Virgo-KAGRA

$$M = M_0 * (1+z)$$

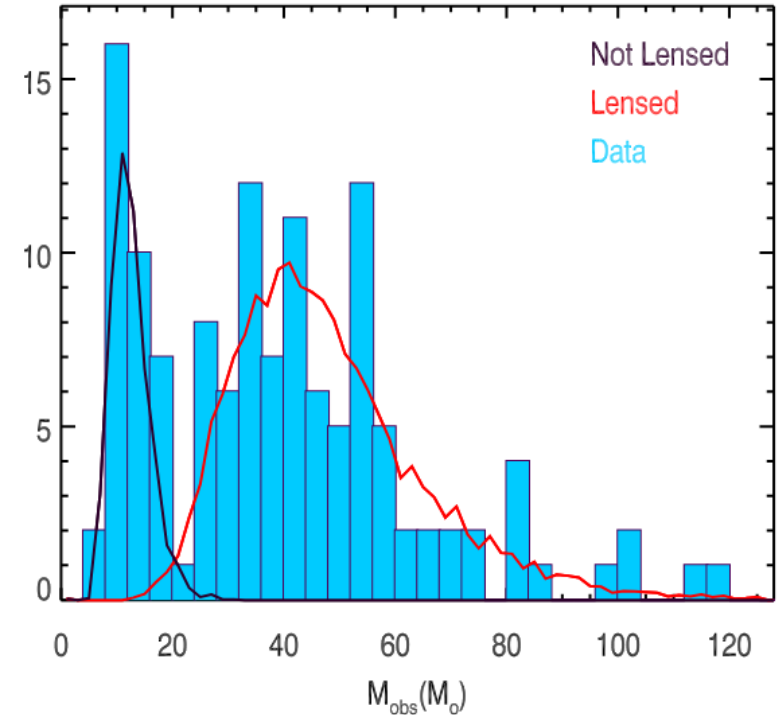
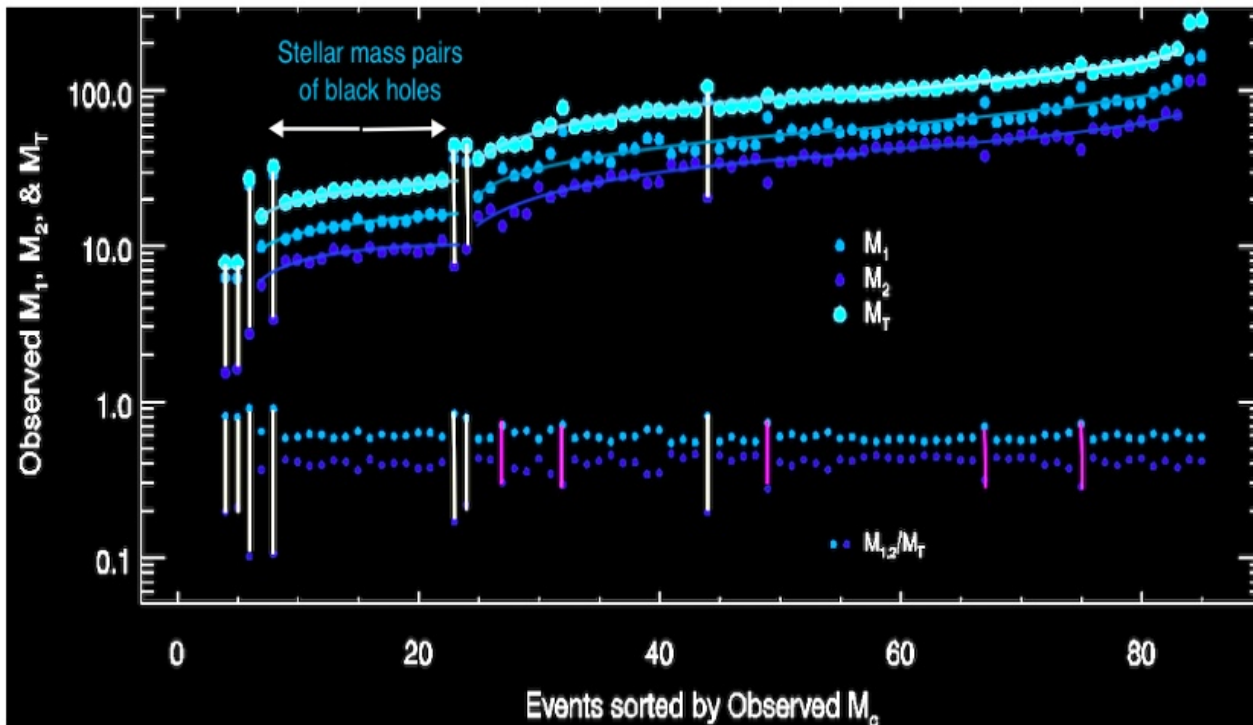
&

$$N = R(z) * V(z) * \tau(>\mu) \sim 10 \text{ yr}^{-1}$$

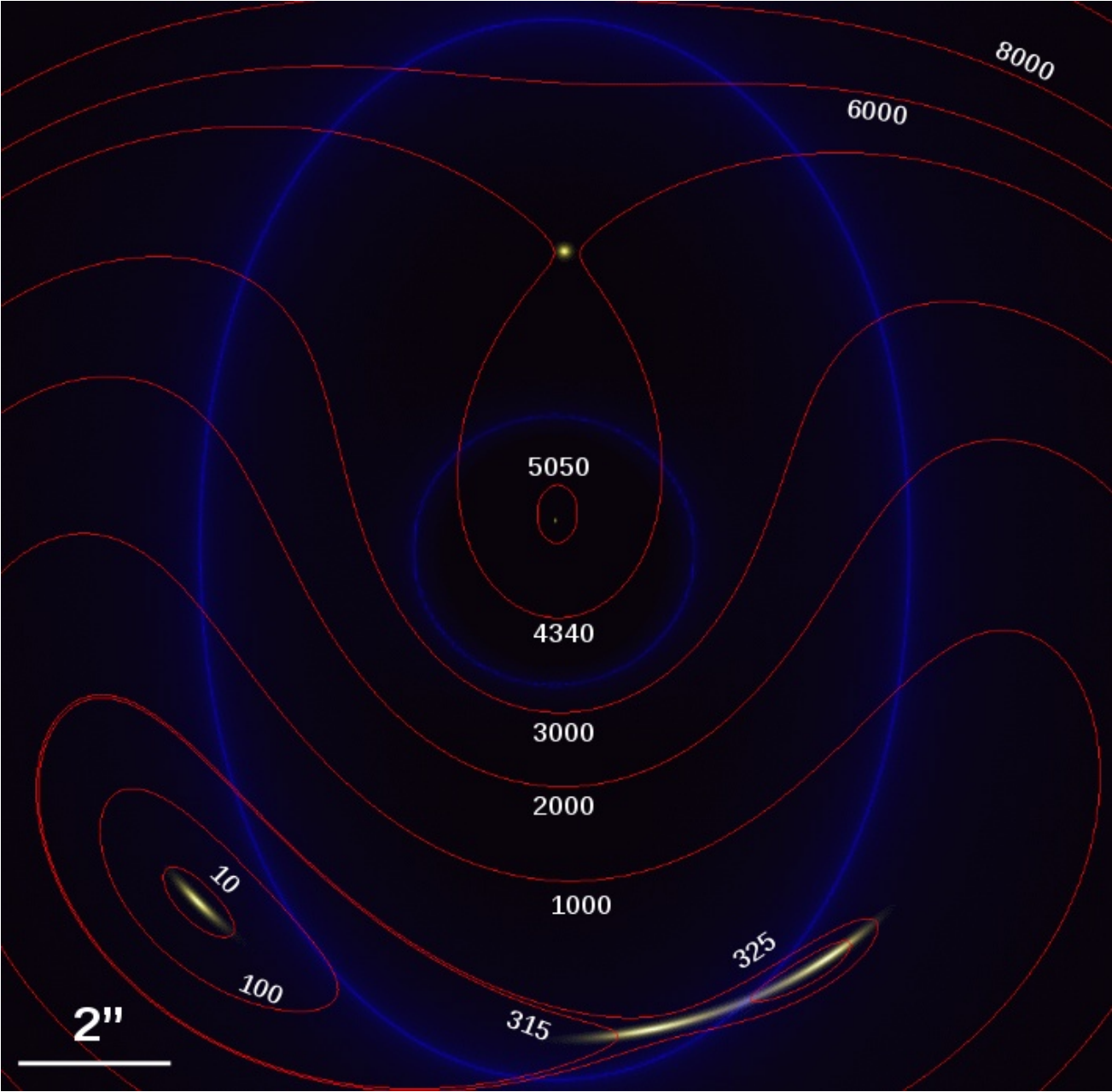
$\sim 10^4 \text{ Gpc}^{-3} \text{ yr}^{-1}$ at $z \sim 2$?

$\sim 500 \text{ Gpc}^3$ between $2 < z < 3$

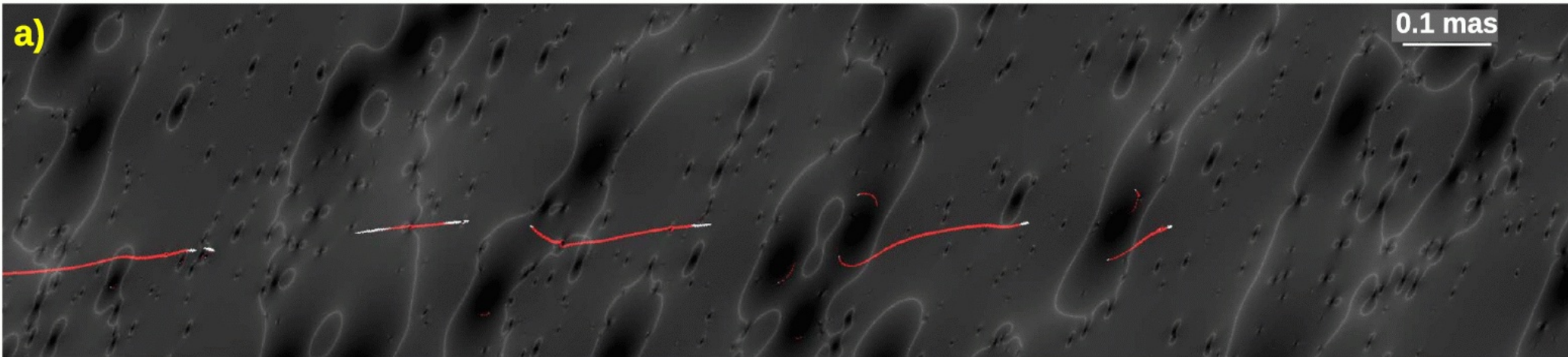
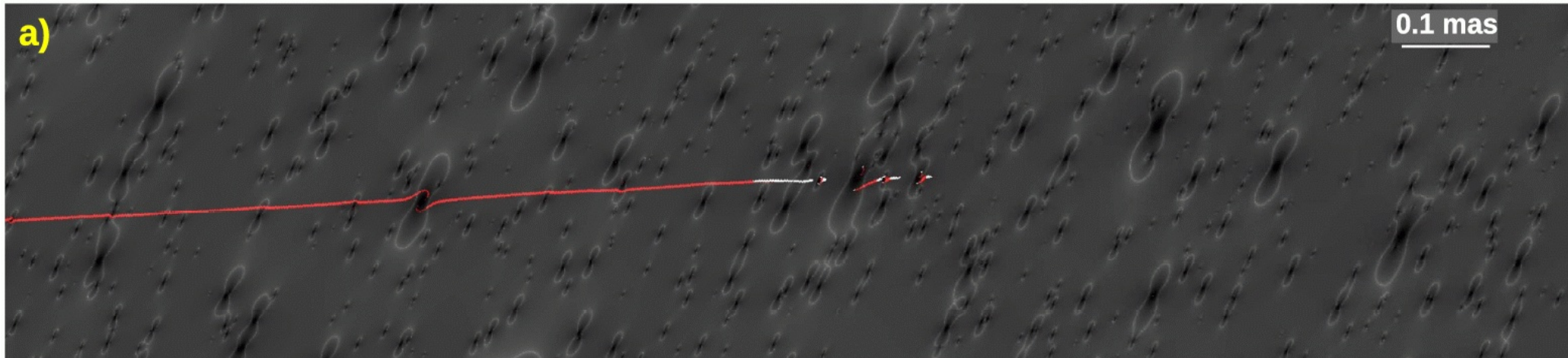
$\sim 10^{-6}$ for $\mu > 50$ at $z \sim 2$?



Time delays at high magnification



Formation and destruction of microimages



More videos in <https://cosmicspectator.org/> (June 2017 post)

- 1- Talk about observations of stars at high- z thanks to gravitational lensing effect, including Earendel. But first a few key ideas about lensing
- 2- Molten Ring. Focus few characteristics.
- 3- Multiple images
- 4- Maximum magnification near CCs
- 5- High- μ and double images. Microlens
- 6- Microlenses ICL lower μ
- 7- Smooth vs Smooth+Micro. μ -Mass
- 8- CC distortions with κ . $\mu \cdot \kappa$
- 9- Neg vs Pos and saturation
- 10- PDF. μ - μ , LogNormal
- 11- Microcaustic network.
- 12- Smooth vs Real
- 13- Mountain climb

-
- 14- Reion.. $z > 6$. BrightStars. Combination3
 - 15- Icarus. Fits star at $z > 1$. $\mu \sim 1000$
 - 16- Microlenses responsible flux change.
PBH and DM (Oguri)
 - 17- First SED of a single star at $z > 1$
 - 18- Godzilla. First star at $z > 2$.
 - 19- No multiple images & unresolved
 - 20- Godzilla must be a star at the CC
 - No time delay explanation (SN)
 - No globular cluster
 - 21- Need a perturber. Dwarf gal.

- 22- Spectrum from MUSE provides more clues
 - Similar to stars like Eta Carinae
 - P-Cygni profile.
 - Great Eruption would explain Godzilla's flux
- 23- Earendel. Farthest star ever seen.
Several lens models agree
Like Godzilla, only one image
Size must be small
- 24- Mass > 50 and $T > 10K$
star might disappear in next 10-30 years
- 25- First SED of a $z > 6$ star
- 26- EIMundoToday
- 27- Windhorst2018. ~ 1 in 3 clusters will show
- 28- Conclusions. LIGO?
- 29 LIGO & Lensing